

Title

A major locus involved in the formation of the radial oxygen loss barrier in adventitious roots of teosinte *Zea nicaraguensis* is located on the short-arm of chromosome 3

Authors and affiliations

Kohtaro Watanabe¹, Hirokazu Takahashi¹, Saori Sato¹, Shunsaku Nishiuchi¹, Fumie Omori², Al Imran Malik³, Timothy David Colmer^{4,5}, Yoshiro Mano^{2,*} & Mikio Nakazono^{1,4,*}

1. Graduate School of Bioagricultural Sciences, Nagoya University, Furo-cho, Chikusa, Nagoya 464-8601, Japan
2. Forage Crop Research Division, Institute of Livestock and Grassland Science, NARO, 768 Senbonmatsu, Nasushiobara, Tochigi 329-2793, Japan
3. Centre for Plant Genetics and Breeding, School of Plant Biology, The University of Western Australia, 35 Stirling Highway, Crawley, WA 6009, Australia
4. School of Plant Biology, The University of Western Australia, 35 Stirling Highway, Crawley, WA 6009, Australia
5. The UWA Institute of Agriculture, The University of Western Australia, 35 Stirling Highway, Crawley, WA 6009, Australia

* Correspondence:

Y. Mano. mano@affrc.go.jp / M. Nakazono. nakazono@agr.nagoya-u.ac.jp

Short running title

Chromosomal region endowing a root ROL barrier

Abstract

1 A radial oxygen loss (ROL) barrier in roots of waterlogging-tolerant plants
2 promotes oxygen movement via aerenchyma to the root tip, and impedes soil phytotoxin
3 entry. The molecular mechanism and genetic regulation of ROL barrier formation are
4 largely unknown. *Zea nicaraguensis*, a waterlogging-tolerant wild relative of maize (*Z.*
5 *mays* ssp. *mays*), forms a tight ROL barrier in its roots when waterlogged. We used *Z.*
6 *nicaraguensis* chromosome segment introgression lines (ILs) in maize (inbred line
7 Mi29) to elucidate the chromosomal region involved in regulating root ROL barrier
8 formation. A segment of the short-arm of chromosome 3 of *Z. nicaraguensis* conferred
9 ROL barrier formation in the genetic background of maize. This chromosome segment
10 also decreased apoplastic solute permeability across the hypodermis/exodermis.
11 However, the IL and maize were similar for suberin staining in the
12 hypodermis/exodermis at 40 mm and further behind the root tip. *Z. nicaraguensis*
13 contained suberin in the hypodermis/exodermis at 20 mm and lignin at the epidermis.
14 The IL with ROL barrier, however, did not contain lignin in the epidermis. Discovery of
15 the *Z. nicaraguensis* chromosomal region responsible for root ROL barrier formation
16 has improved knowledge of this trait and is an important step towards improvement of
17 waterlogging tolerance in maize.

18

Keywords

20 aerenchyma, crop flooding tolerance, introgression lines, lignin, maize, radial oxygen
21 loss barrier, suberin, waterlogging tolerance, *Zea nicaraguensis*

22 **Introduction**

23 During periods of waterlogging, non-wetland plants such as maize (*Zea mays* ssp.
24 *mays*), wheat (*Triticum aestivum*) and barley (*Hordeum vulgare*) suffer from oxygen
25 deficiency (Bailey-Serres *et al.* 2012) and from exposure to phytotoxic products of
26 anaerobic metabolism by microorganisms in the soil (Chandrasekaran & Yoshida 1973;
27 Kirk *et al.* 2014). Wetland plants have several traits that enable them to cope with
28 long-duration soil waterlogging, but these are less developed or in some cases absent in
29 dryland species. These traits include: formation of aerenchyma which enhances internal
30 movement of oxygen; development of a radial oxygen loss (ROL) barrier in roots to
31 restrict oxygen leakage radially from aerenchyma to the rhizosphere in basal zones;
32 emergence of adventitious roots (often near, or on, the soil surface); tolerance of toxic
33 soil constituents, such as Fe²⁺ (Armstrong *et al.* 1994; Colmer & Voesenek 2009; Kirk
34 *et al.* 2014; Voesenek & Bailey-Serres 2015).

35 Many waterlogging-tolerant plants, such as rice (*Oryza sativa*), *Phragmites*
36 *australis* and *Hordeum marinum*, constitutively form aerenchyma under well-drained or
37 well-aerated conditions (constitutive aerenchyma formation) and the amount of
38 aerenchyma is further induced under waterlogged or oxygen-deficient conditions
39 (inducible aerenchyma formation) (Justin & Armstrong 1987; Malik *et al.* 2011; Shiono
40 *et al.* 2011). Moreover, some waterlogging-tolerant plants develop a ROL barrier in the
41 outer cell layers of the basal zone of roots (Armstrong 1979); these roots contain
42 hypodermis/exodermis and in some species (e.g. rice) also sclerenchyma. Under
43 stagnant deoxygenated conditions in a nutrient solution, which mimics the changes in
44 gas composition in waterlogged soil, the ROL barrier enhances longitudinal oxygen
45 diffusion to the root tip of rice and various other wetland species (Armstrong 1979;

46 Colmer 2003a, b; Soukup *et al.* 2007; Kotula *et al.* 2009a; Malik *et al.* 2011; Shiono *et*
47 *al.* 2011). Hence, the combination of aerenchyma and a ROL barrier greatly improve the
48 supply of oxygen to the tips of roots in waterlogged soil (Armstrong 1979; Colmer &
49 Voesenek 2009).

50 Recent studies have elucidated ROL barrier formation in rice roots. Although
51 ethylene enhances aerenchyma formation and adventitious root emergence, it does not
52 induce ROL barrier formation (Colmer *et al.* 2006). Hypodermal/exodermal cell walls
53 develop novel electron-dense materials during ROL barrier formation (Shiono *et al.*
54 2011). The biopolymers suberin and lignin accumulate in the cell walls in the outer part
55 of roots (Kotula *et al.* 2009a; Ranathunge *et al.* 2011) [as well as in the roots of *P.*
56 *australis* (Armstrong *et al.* 2000; Soukup *et al.* 2007)] grown under waterlogged
57 conditions, so these cell wall modifications have been associated with ROL barrier
58 formation. A transcriptome analysis using laser-microdissected tissues of the outer cell
59 layers of rice roots revealed that many genes involved in suberin biosynthesis (but not
60 lignin biosynthesis) were strongly up-regulated during ROL barrier formation (Shiono
61 *et al.* 2014b). However, the mechanism of the root ROL barrier formation remains
62 unclear. One approach to elucidate the genes involved in ROL barrier formation is to
63 use a forward genetics approach, in which a chromosomal region of interest is identified,
64 e.g., by examining chromosome segment introgression lines (ILs) with different
65 phenotypes.

66 To improve the ability of various crops to tolerate biotic and abiotic stresses, wild
67 relatives of crops can be a valuable germplasm resource. *Zea nicaraguensis* (Nicaraguan
68 teosinte, Iltis & Benz 2000), a wild relative of maize, has been considered as a genetic
69 resource because of its high waterlogging-tolerance (Mano & Omori 2007; Mano *et al.*

70 2016). *Z. nicaraguensis* is able to form constitutive and inducible aerenchyma, whereas
71 maize does not form constitutive aerenchyma (e.g. Abiko *et al.* 2012; Mano & Omori
72 2013a, b). Moreover, *Z. nicaraguensis* induces the formation of a tight ROL barrier in
73 roots under stagnant deoxygenated conditions, but not under aerobic conditions,
74 whereas maize does not form a tight ROL barrier under either aerobic or stagnant
75 deoxygenated conditions (Abiko *et al.* 2012). *Z. nicaraguensis* is also superior to maize
76 in forming surface (i.e. above-ground) adventitious roots (Mano *et al.* 2009) and in
77 tolerating reduced soil redox conditions (Mano & Omori 2013a). Some of these traits,
78 such as formation of constitutive aerenchyma, development of surface adventitious
79 roots and tolerance of reduced soil redox, are heritable in the progeny of the crosses
80 between maize and *Z. nicaraguensis* (Mano *et al.* 2016). This means that *Z.*
81 *nicaraguensis* can be used as a genetic resource to improve waterlogging tolerance in
82 maize, which would be most efficient using DNA marker-assisted selection. For this
83 purpose, several quantitative trait loci (QTLs) that are involved in waterlogging
84 tolerance have been identified by analyses of mapping populations and ILs derived from
85 crosses between maize (inbred line Mi29) and *Z. nicaraguensis* (summarized in Mano *et*
86 *al.* 2016). However, so far, no QTLs associated with root ROL barrier formation have
87 been identified in any plant species. Thus, *Z. nicaraguensis*, which displays a tight root
88 ROL barrier, a feature lacking in maize (Abiko *et al.* 2012), should be a useful parent
89 for developing a population of chromosome segment ILs in maize with the aim to
90 identify QTL(s) for the root ROL barrier trait.

91 In this study, we identified the chromosomal region involved in the formation of a
92 root ROL barrier using a series of ILs, each possessing a chromosome segment from *Z.*
93 *nicaraguensis* in the genetic background of maize inbred line Mi29 (Fig. S1; Mano &

94 Omori 2013a). We also investigated whether this chromosome segment alters the
95 accumulation of suberin or lignin in the outer part of the roots and if ROL barrier
96 formation alters the permeability to solutes across the apoplast of the outer part of the
97 roots. The identification of the chromosomal region of *Z. nicaraguensis* that controls the
98 ROL barrier in roots is an important step in a forward genetics approach towards
99 discovery of the gene(s) regulating this trait and towards improvement of waterlogging
100 tolerance in maize.

101

102 **Materials and Methods**

103

104 ***Plant materials***

105 Maize (*Zea mays* ssp. *mays*) inbred line Mi29 developed at the Kyushu Okinawa
106 Agricultural Research Center, NARO, Japan (Ikegaya *et al.* 1999b) was obtained from
107 the Institute of Livestock and Grassland Science, NARO, Japan, and *Zea nicaraguensis*
108 (CIMMYT 13451) was provided by the International Maize and Wheat Improvement
109 Center (CIMMYT), Mexico. A series of introgression lines (ILs) each possessing a
110 chromosome segment from *Z. nicaraguensis* in the genetic background of maize inbred
111 line Mi29 were developed (Fig. S1; Mano & Omori 2013a) and used. Of 45 ILs, we
112 evaluated a total of 42 ILs because of the limitation of seed number in IL#17, IL#20 and
113 IL#40. We also used four additional lines obtained during the development of IL#11 and
114 IL#42. These four additional lines consist of #418 (possesses segments of chromosomes
115 1 and 4 of *Z. nicaraguensis*), #422 (possesses segment of chromosome 4 of *Z.*
116 *nicaraguensis*), #426 (possesses segments of chromosomes 3 and 4 of *Z. nicaraguensis*)
117 and #468 (possesses segments of chromosomes 3, 9 and 10 of *Z. nicaraguensis*); all in

118 the genetic background of maize inbred line Mi29 (Fig. 3A).

119

120 ***Growth conditions***

121 To sterilize and align the timing of germination, seeds were treated with a 10%
122 (v/v) solution of hydrogen peroxide for 2 min (Naredo *et al.* 1998). The seeds were then
123 thoroughly rinsed with deionized water and were placed at the upper end within a roll of
124 wet filter paper (30 × 26 cm). The rolled papers were transferred into 2 L plastic pots
125 with 200 mL deionized water with the base of the rolled papers in the water. The pots
126 were shaded by wrapping with aluminum foil so that the seeds were in the dark, and the
127 pots were placed into a growth chamber (LH-411SP; Nippon Medical & Chemical
128 Instruments Co., Ltd, Osaka, Japan) for 4 days at 28°C. On the fourth day, seedling
129 shoots had emerged above the filter paper roll and the aluminum foil cover was
130 removed to expose the shoots to light (PAR of 250-300 $\mu\text{mol m}^{-2} \text{s}^{-1}$; 14 h light/10 h
131 dark) for 1 day. Five-day-old seedlings were transferred to 5 L pots (4 plants per pot)
132 containing half-strength nutrient solution, and grown hydroponically with aeration for 6
133 days. The composition of the nutrient solution at full strength was 1.0 mM NH_4NO_3 ,
134 0.50 mM NaH_2PO_4 , 0.30 mM K_2SO_4 , 0.30 mM CaCl_2 , 0.60 mM MgCl_2 , 45 μM
135 Fe-EDTA, 50 μM H_3BO_3 , 9.0 μM MnSO_4 , 0.30 μM CuSO_4 , 0.70 μM ZnSO_4 , 0.10 μM
136 Na_2MoO_4 (Mae & Ohira 1981). The nutrient solution also contained 5.0 mM
137 2-(*N*-morpholino)ethanesulfonic acid (MES) buffer and the pH was adjusted to 5.5
138 using KOH (Abiko *et al.* 2012). To avoid iron deficiency in the young seedlings when
139 in aerated solution, 1 ml of freshly made 25 mM FeSO_4 was added per pot to provide a
140 final Fe^{2+} concentration of 5.0 μM every 2 days (Kulichikhin *et al.* 2014). When
141 seedlings were 11-day-old, the solution was changed to stagnant deoxygenated nutrient

142 solution, which contained the same half-strength nutrient solution as described above
143 and 0.1% (w/v) agar; this solution was deoxygenated by bubbling with nitrogen gas
144 (Wiengweera *et al.* 1997). The dissolved oxygen level was lower than 0.5 mg L⁻¹
145 (quantification used a dissolved oxygen meter; SevenGo pro-SG6, Mettler Toledo,
146 Schwerzenbach, Switzerland). The stagnant deoxygenated nutrient solution was
147 renewed each 7 days. To prevent entry of light to the roots the pots were wrapped with
148 aluminum foil and the surface of the foam float, which held each plant at the shoot base,
149 was also covered on the top-side with aluminum foil. Adventitious roots of 25- to
150 27-day-old plants were used to evaluate root ROL barrier formation, histochemical
151 staining of suberin and lignin, and solute permeability. Adventitious roots measured had
152 emerged after transfer of the plants to a stagnant deoxygenated solution.

153

154 *Assessments of spatial patterns of radial oxygen loss (ROL) from adventitious roots*
155 *when in an oxygen-free medium*

156 ROL barrier formation in roots was evaluated using two methods: (1) methylene
157 blue staining and (2) measurement of ROL by root-sleeving cylindrical platinum oxygen
158 electrodes, in both cases for roots in a deoxygenated medium and reliant on internal
159 oxygen movement from the shoots in air.

160 (1) Method for methylene blue staining. Methylene blue, which is a redox indicator
161 dye, enables qualitative assessments of spatial ROL profiles from roots (Armstrong &
162 Armstrong 1988; Armstrong *et al.* 1992; Kotula & Steudle 2009; Shiono *et al.* 2011).
163 The reduced form of methylene blue is colorless, whereas the oxidized form is blue.
164 This visual method enabled us to screen the large number of ILs for patterns of ROL
165 along roots. Methylene blue was at 13 mg L⁻¹ in a deoxygenated solution containing

166 0.1% (w/v) agar, and sodium dithionite ($\text{Na}_2\text{S}_2\text{O}_4$) was at 130 mg L^{-1} in order to reduce
167 the methylene blue so that it was colorless. Plants used were 25-day-old and to aid
168 visualization one root per plant with a length of 60 mm or greater (except for IL#6 with
169 ave. 59 mm and IL#35 with ave. 48 mm lengths) was selected, and all other roots were
170 trimmed off immediately prior to use. Plants were transferred to the methylene blue
171 solution in an acrylic tank and held with the root-shoot junction positioned at 30 mm
172 below the surface of the solution. The tank was at room temperature ($\sim 25^\circ\text{C}$) under the
173 white light inside the laboratory. After 15-20 min, the staining patterns of methylene
174 blue around the roots of 3 or 4 plants of each IL, and the parents, were evaluated.

175 (2) Method for ROL measurement using a root-sleeving oxygen electrode.
176 Root-sleeving (i.e. cylindrical platinum) oxygen electrodes enable quantification of
177 ROL at selected positions along roots when in an oxygen-free medium (Armstrong &
178 Wright 1975). The intact roots (i.e. all roots intact) of 25- to 27-day-old plants were
179 immersed in deoxygenated solution containing 0.1% (w/v) agar, 5.0 mM KCl and 0.50
180 mM CaSO_4 (Colmer *et al.* 1998). For deoxygenation, the solution had been bubbled
181 with high-purity nitrogen gas. Each plant was held with the root-shoot junction at 30
182 mm below the surface of the oxygen-free medium in an acrylic tank and the shoot was
183 in air, all at 28°C in a growth chamber with conditions the same as during plant growth.
184 A cylindrical platinum electrode (inner diameter 2.25 mm, height 5.0 mm) fitted with
185 root-centralizing guides was placed around a selected adventitious root (90-140 mm in
186 length). The cylindrical platinum electrode was polarized relative to a
187 silver/silver-chloride reference. Voltage was adjusted with a potentiostat
188 (HA-1010mM1A, Hokuto Denko co., Tokyo, Japan) to obtain a current near the peak of
189 the current voltage curve. Voltage and current outputs from the potentiostat were

190 monitored with a laptop computer with the custom-made software. The ROL
191 measurements were taken along each root by positioning the center of the electrode at
192 distances of 5, 10, 20, 30, 40, 50, 60, 70 and 80 mm behind the root tip. Measurements
193 were taken below the zone with lateral roots, so these did not affect the patterns of ROL
194 measured along of the roots, but laterals can influence the amounts of ROL from apical
195 portions (see Discussion). Differences in lateral roots did not affect our goal to identify
196 whether, or not, roots of various genotypes could, or could not, form a tight barrier to
197 ROL in the main axis of adventitious roots.

198 The diagnostic feature for roots with a tight barrier to ROL for methylene blue
199 staining along roots in an oxygen-free medium, and of ROL measured with the
200 root-sleeving oxygen electrode, are summarized in the Results.

201

202 ***Measurement of adventitious root porosity***

203 The porosity (% gas volume per unit tissue volume) of adventitious roots was
204 determined using the method described by Raskin (1983) and the equations as modified
205 by Thomson *et al.* (1990). Measurements were taken for adventitious roots of 50-100
206 mm in length without any laterals.

207

208 ***Preparation of cross sections for histochemical analyses***

209 Root cross-sections were prepared from 10 mm-long root segments excised from
210 adventitious roots (lengths, 90-140 mm). Root segments were sampled at distances of
211 5-15, 15-25, 25-35, 35-45, 45-55, 55-65, 65-75 and 75-85 mm behind the root tip. The
212 segments were embedded in 4% (w/v) agar. Cross-sections were made by cutting agar
213 blocks containing root segments using a vibrating microtome (VT 1200S; Leica

214 Biosystems Nussloch GmbH, Nussloch, Germany) at 75 µm thickness. To remove the
215 adherent agar from the sections, they were incubated with clearing solution (2 g mL⁻¹
216 chloral hydrate in glycerol:water = 1:3) for 1 hour at 70°C. After clearing, the
217 cross-sections were washed several times with warm water and then stained as
218 described in the next section.

219

220 ***Histochemical staining of suberin and lignin***

221 Suberin lamellae of root cross-sections were detected using Fluorol Yellow 088.
222 The staining solution was prepared by adding Fluorol Yellow 088 in polyethylene glycol
223 400 (PEG-400) at 0.1% (w/v), dissolving with heating at 90°C for 1 hour, and then
224 adding 90% glycerol at the same volume as the PEG-400 (Brundrett *et al.* 1991; Lux *et*
225 *al.* 2005). The cleared root cross-sections were placed in the staining solution for 1 hour
226 at room temperature. Excess stain was washed away by several rinses with warm water.
227 Suberin lamellae were detected with a CCD camera (DP70, Olympus Optical Co. Ltd.,
228 Tokyo, Japan) as yellow fluorescence upon excitation by UV light (U-RFL-T, Olympus
229 Optical Co. Ltd.) under a fluorescence microscope (Olympus BX60) equipped with
230 U-MWU filter cube (Olympus Optical Co. Ltd.).

231 Lignin in root cross-sections was detected by phloroglucinol/HCl staining (Jensen
232 1962). The staining solution was prepared as 1% (w/v) by adding phloroglucinol in 75%
233 ethanol. The cleared root cross-sections were soaked in staining solution for 1 hour and
234 then dipped in 6 M HCl for 10 min, and then observed. Lignified tissues were stained
235 red when visualized under white light.

236

237 ***Permeability test***

238 The permeability of hypodermal/exodermal cell layers of roots was assessed using
239 periodic acid-Schiff (PAS) staining. PAS staining is preferred to some other apoplastic
240 tracers because periodic acid reacts with cell wall polysaccharides to create dialdehydes
241 from diols of polysaccharidic rings and then the dialdehydes react with the Schiff
242 reagent to give a purple-magenta color, which does not diffuse or get washed out during
243 sample processing (Pecková *et al.* 2016). Adventitious roots (lengths, 90-140 mm) were
244 sampled and the cut basal end was covered with petroleum jelly in order to prevent the
245 influx of periodic acid solution via the cut end. The roots were incubated in 0.1% (w/v)
246 H₅IO₆ for 1 hour and washed with reducing solution containing 2% (w/v) KI and 2%
247 (w/v) Na₂S₂O₃·5H₂O for 1 hour. After incubation and washing, roots were embedded in
248 4% (w/v) agar and cross-sections were made using a vibrating microtome (VT 1200S;
249 Leica Biosystems Nussloch GmbH) at 150 µm thickness. The cross-sections of the roots
250 were stained in Schiff's reagent for 10 min. The penetrated periodic acid was visualized
251 as purple staining in the cell walls when observed under a light microscope.

252

253 *Statistical analysis*

254 Data are presented as the mean ± standard deviation. Comparisons of means were
255 at a confidence level of 90% using one-way ANOVA and then Dunnett's test.

256

257 **Results**

258

259 *ROL barrier formation in adventitious roots*

260 To determine the chromosomal region that is responsible for root ROL barrier
261 formation in *Z. nicaraguensis*, we used a series of ILs, each containing a chromosome

262 segment (or in some cases segments) from *Z. nicaraguensis* in the maize inbred line
263 Mi29, which cover nearly the entire genome of *Z. nicaraguensis* (Fig. S1). The
264 locations of ROL from roots in oxygen-deficient media can be visualized by staining
265 with methylene blue. We used this approach to screen for ROL barrier formation in
266 adventitious roots of maize, *Z. nicaraguensis* and the ILs when grown under stagnant
267 deoxygenated conditions. Roots containing oxygen, and without a ROL barrier would
268 appear blue (i.e. show the presence of oxygen) along much of their length and especially
269 in the more basal zones closer to the root/shoot junction where internal oxygen
270 concentration is highest. By contrast, roots containing oxygen and with a ROL barrier
271 would lack or only show slight blue coloration along the basal portions, but the tip
272 region would be blue.

273 In maize, the entire root from the base to the apex was stained blue by 15-20 min
274 after transfer into the assay medium (Fig. 1A), and subsequently blue halos were formed
275 around the entire length of the root (own observations). By contrast, for *Z.*
276 *nicaraguensis* roots, only the apical portion (<20 mm from the tip) strongly stained blue,
277 while the remainder of the root (>20 mm from the tip) was only weakly stained (Fig.
278 1A), and subsequently a blue halo formed around only the apical portion of the root
279 (own observations). These markedly different ROL profiles of maize and *Z.*
280 *nicaraguensis* were confirmed by measurements taken with a root-sleeving oxygen
281 electrode at different distances behind the root apex of adventitious roots. In maize,
282 ROL was high (about $100 \text{ nmol m}^{-2} \text{ s}^{-1}$) at all positions from 5 to 80 mm from the root
283 tip (Fig. 1B), indicating only a weak (but not tight) ROL barrier at basal regions in
284 maize adventitious roots. On the other hand, for *Z. nicaraguensis*, ROL at the basal and
285 middle parts (i.e. 40-80 mm behind the tip) of adventitious roots was very low but it

286 was high in the apical parts (i.e. 5-30 mm behind the tip). This distinct pattern confirms
287 that *Z. nicaraguensis* forms a tight ROL barrier at mid-to-basal zones of adventitious
288 roots, when grown in stagnant deoxygenated conditions.

289 The methylene blue staining assay to visualize root ROL patterns was used to
290 screen the available 42 ILs to determine if any of these can form a tight ROL barrier
291 when grown in stagnant deoxygenated solution. All of the ILs, with the exception of
292 IL#11, showed oxygen staining along the entire length of their roots, a pattern similar to
293 that of maize, whereas IL#11 (3 plants out of 4 plants tested) showed a ROL staining
294 pattern similar to that of *Z. nicaraguensis* (Fig. 2). The ROL staining patterns of the
295 main axes were consistent along the measured roots of 3 or 4 plants of each IL, even
296 though the numbers and lengths of lateral roots in the basal zones sometimes differed
297 amongst individual roots (own observations). Moreover, the root-sleeving electrode
298 measurements along adventitious roots of IL#11 also found that ROL was very low at
299 mid-to-basal parts (i.e. 30-80 mm behind the root tip), but was much higher in the apical
300 part (i.e. 5-20 mm behind the root tip), as it was in *Z. nicaraguensis* (see Fig. 4). These
301 results indicated that IL#11 has an ability to form a tight ROL barrier in the basal zones.

302

303 ***The chromosome segment responsible for root ROL barrier formation***

304 IL#11 possessed three chromosome segments of *Z. nicaraguensis* from
305 chromosomes 1, 3 and 4, in the genetic background of maize (Fig. 3A). To identify the
306 chromosomal segment(s) that contribute to tight ROL barrier formation in roots, we
307 evaluated four additional ILs obtained during the development of IL#11 and IL#42, as
308 these had different combinations of the three chromosome segments in IL#11. These
309 consist of sibling (sister) lines of IL#11 (#418, #422 and #426) and IL#42 (#468) (Fig.

310 3A).

311 For the adventitious roots of lines #418, #422 and IL#42, as for those of maize, the
312 whole root length stained blue in the methylene blue assay (Fig. 3B) and measurements
313 with the root-sleeving electrode indeed showed that ROL was high from all positions at
314 5 to 80 mm behind the root tip of these three lines (Fig. 4). By contrast, adventitious
315 roots of lines #426 and #468 only stained blue for the tip region (0-20 mm) of the root
316 (Fig. 3B). Moreover, the root-sleeving electrode measurements along adventitious roots
317 of lines #426 and #468 (as well as IL#11), showed that ROL was very low at 30-80 mm
318 from the root tips, but was much higher in the apical region (5-20 mm behind the root
319 tip) (Fig. 4); such patterns of root ROL resemble those of *Z. nicaraguensis* (Fig. 1).
320 These results that line #418, line #422 and IL#42, like maize, all form only a weak ROL
321 barrier, whereas lines #426 and #468 form a tight ROL barrier, implicate the segment
322 from the short-arm of chromosome 3 of *Z. nicaraguensis* in conferring this trait of a
323 tight ROL barrier in basal zones of roots when in stagnant deoxygenated conditions.

324 Although the patterns of ROL showed that IL#11 and lines #426 and #468 can all
325 form a tight ROL barrier, the ROL amounts just behind the apex (i.e. at 5 mm) in these
326 three lines were all slightly lower (Fig. 4) than those for roots of *Z. nicaraguensis* (Fig.
327 1B). To determine whether the higher ROL from the apical region of *Z. nicaraguensis*
328 roots could be due to a greater gas-filled porosity than in the ILs, we measured porosity
329 (% gas volume/root volume) of the adventitious roots of a sub-set of relevant genotypes
330 (both parents, two lines with the chromosome 3 segment from *Z. nicaraguensis* and one
331 line without the segment). We found that *Z. nicaraguensis* roots were of higher porosity,
332 being 26% as compared with 19% in maize and 15-19% in the three ILs measured (two
333 with tight ROL barrier: IL#11 and line #468; one with weak ROL barrier: IL#42) (Fig.

334 S2).

335 In IL#11 (which can form a tight ROL barrier), the *Z. nicaraguensis*-derived
336 segment on chromosome 3 was heterozygous (Fig. 3A), suggesting the region was
337 segregating in individual plants of IL#11 (being homozygous and heterozygous for *Z.*
338 *nicaraguensis* in some plants and homozygous for maize in other plants). To verify the
339 location on chromosome 3, we evaluated 10 of the IL#11 plants with known genotypes
340 in this region, for root ROL patterns using the methylene blue staining assay. The plants
341 possessing the *Z. nicaraguensis*-derived chromosome 3 segment with homozygotes and
342 heterozygotes formed a tight ROL barrier at the mid-to-basal parts of adventitious roots,
343 whereas those possessing the maize-derived segment did not (Fig. S3), indicating that
344 the gene(s) involved in ROL barrier formation on this segment of chromosome 3 of *Z.*
345 *nicaraguensis* is dominant.

346

347 ***Suberin and lignin staining of root cross-sections***

348 To investigate whether the segment of *Z. nicaraguensis* chromosome 3 involved in
349 root ROL barrier formation influences accumulation of suberin or lignin in the outer
350 part of the roots, we stained for these two substances in root cross-sections. We
351 examined line #468 which contains the *Z. nicaraguensis* chromosome 3 segment and
352 IL#42 which lacks the segment, as well as maize and *Z. nicaraguensis*. Suberin was
353 observed in the outer cell layers at 40-80 mm from the root tips in maize, line #468 and
354 IL#42, and at 20-80 mm from the root tips in *Z. nicaraguensis* (Fig. 5). Lignin was
355 observed at the epidermis at 20-80 mm from the root tips in *Z. nicaraguensis* roots, but
356 not in the epidermis at any parts of roots of maize, line #468 and IL#42 (Fig. 6). These
357 results indicate that the segment of chromosome 3 from *Z. nicaraguensis* which confers

358 the root ROL barrier trait, is not simply related to changes in suberin or lignin
359 accumulation in the outer cell layers as detected using these histochemical staining
360 techniques.

361

362 ***Permeability of adventitious roots***

363 To examine whether the segment of *Z. nicaraguensis* chromosome 3 involved in
364 root ROL barrier formation also results in a changed solute permeability across the outer
365 part of the root, we investigated penetration of periodic acid across the
366 hypodermal/exodermal layers of adventitious roots of maize, *Z. nicaraguensis*, line
367 #468 (with segment) and IL#42 (without segment). In maize and IL#42, periodic acid
368 penetrated the outer cell layers and reached the internal tissues (i.e. cortex) at all
369 positions from 10 to 80 mm behind the root tips, whereas in *Z. nicaraguensis* and line
370 #468, penetration was blocked at the hypodermis/exodermis at positions 30-80 mm
371 behind the root tips (Fig. 7). This result indicates that the latter two genotypes, both of
372 which possess a tight ROL barrier in the roots, had both formed an apoplastic barrier to
373 solutes in these same mid-to-basal regions along the roots from which ROL is low.

374

375 **Discussion**

376

377 In this study, we used a forward genetics approach to improve understanding of the
378 mechanism of ROL barrier formation in roots as an acclimation to waterlogging stress.
379 To this end, we focused on two contrasting *Zea* species because of the presence of
380 variation within the genus for this trait: formation of a tight ROL barrier is induced in *Z.*
381 *nicaraguensis* roots, but not in *Zea mays* ssp. *mays* (maize) roots, under stagnant

382 deoxygenated conditions (Abiko *et al.* 2012; present study). These two *Zea* species can
383 be crossed and the progeny can be used for genetic analyses. In addition, a series of ILs
384 each possessing a chromosome segment (or segments) from *Z. nicaraguensis* in the
385 genetic background of maize inbred line Mi29 had been developed (Mano & Omori
386 2013a), which cover nearly the entire genome of *Z. nicaraguensis* (in 45 ILs). IL#11
387 was found to form a root ROL barrier (Fig. 2) and the chromosomal region related to
388 ROL barrier formation was identified (Fig. 3). However, the possibility that IL#17,
389 IL#20 and IL#40, which did not produce enough seeds to be examined, have one or
390 more additional loci for ROL barrier formation cannot be ruled out. Among the
391 available 42 ILs, three lines (IL#5, IL#11 and IL#12) have various *Z.*
392 *nicaraguensis*-derived chromosome 3 segments (Figs. S1 & 8), but interestingly of
393 these only IL#11 formed a tight ROL barrier (Fig. 2). These phenotypic results,
394 together with DNA marker analyses of chromosome 3 in these three lines, reveal that
395 the locus/loci controlling root ROL barrier formation is located within a ~22.6 Mb
396 region between DNA markers bnlg1325 and bnlg1113 on the short-arm of chromosome
397 3 of *Z. nicaraguensis* (Fig. 8). Although further fine mapping of the locus/loci for root
398 ROL barrier formation will be necessary for confirming this location and the identity of
399 the gene(s), this is the first study to identify a chromosomal region containing a
400 locus/loci controlling root ROL barrier formation in any species.

401 Formation of aerenchyma and induction of a barrier to ROL enhance oxygen
402 diffusion along roots to the apex of the main axis. The ROL barrier in basal root zones
403 can also impede phytotoxin entry from waterlogged soil as permeability across the
404 hypodermis/exodermis is reduced (e.g. Fig. 7), while ROL from the apical part of the
405 root can oxidize the reduced soil phytotoxins (such as Mn^{2+} , Fe^{2+} and S^{2-}), so together

406 can decrease potential damage to roots (Armstrong 1979; Colmer 2003b). Waterlogging
407 tolerance-related-traits in *Z. nicaraguensis* have been mapped to several chromosomes
408 (see Mano *et al.* 2016), with a QTL associated with tolerance to reduced soil conditions
409 mapped to the long-arm of chromosome 4. The QTL for tolerance of reduced soil
410 conditions on a locus on chromosome 4 was not on the same chromosome as the root
411 ROL barrier trait on chromosome 3, so the two traits appear to be under different
412 genetic control and the mechanism of tolerance to reduced soil remains to be elucidated.
413 Moreover, it might be possible to increase tolerance to reduced conditions in
414 waterlogged soil by combining of the two traits, a breeding process which would be
415 facilitated by use of DNA marker-assisted selection. Similarly, four QTLs for
416 constitutive aerenchyma formation on chromosomes 1 (2 regions), 5 and 8 of *Z.*
417 *nicaraguensis* (Mano & Omori 2008, 2009) were also on different chromosomes to that
418 associated with the root ROL barrier on the short-arm of chromosome 3. The QTL
419 controlling above-ground adventitious root formation during flooding, like the QTL
420 controlling root ROL barrier formation, is located on the short-arm of chromosome 3
421 (Mano *et al.* 2009). Fine-mapping analyses of both traits will be necessary to define the
422 specific locus or loci for each of these two traits on the short-arm of chromosome 3, as
423 well as for the other traits for waterlogging tolerance on the various other chromosomes
424 of *Z. nicaraguensis*.

425 The distinctly different patterns of ROL along the roots identified genotypes with,
426 or without, a root ROL barrier in basal zones (see Results and Discussion above); here
427 we comment on the rates of ROL just behind the root tips. The amount of oxygen
428 reaching the tip of a root reliant on internal oxygen diffusion is determined by several
429 factors including; root porosity, respiratory consumption, ROL and distance (i.e. root

430 length) (Armstrong 1979). Lateral roots contribute to the respiratory consumption of
431 oxygen and so can decrease the amount of oxygen within the main axis (Armstrong *et al.*
432 1983; Sorrell *et al.* 2000) but this effect is lessened the closer that laterals emerge to the
433 root-shoot junction (Armstrong *et al.* 1990). We do not have data on the position,
434 numbers and lengths of lateral roots, so cannot comment further on this aspect for the
435 present genotypes. The root porosities (gas-filled volume per unit root volume) of IL#11
436 (17%) and line #468 (15%) (both have the chromosome 3 segment from *Z.*
437 *nicaraguensis* endowing ROL barrier formation) were comparable to those of maize
438 (19%) and IL#42 (19%) (both lack the chromosome 3 segment from *Z. nicaraguensis*)
439 (Fig. S2). By contrast, the root porosity of 26% in *Z. nicaraguensis* was higher than the
440 15-19% in maize and these three ILs (Fig. S2). The present root porosity data for the ILs
441 support that the loci for the superior aerenchyma formation in *Z. nicaraguensis* are not
442 located on the short-arm of chromosome 3 (four QTLs for constitutive aerenchyma were
443 identified elsewhere, Mano & Omori 2008, 2009). ROL rates just behind the tip of the
444 roots of IL#11 and line #468 (both form a tight ROL barrier) were slightly lower (Fig.
445 4) than from near the tip of roots of *Z. nicaraguensis* (Fig. 1B); the greater root porosity
446 of *Z. nicaraguensis* would result in a higher internal oxygen concentration within these
447 roots (cf. Armstrong 1979). Thus, it is possible to enhance the transport of oxygen to the
448 root apex by combining greater aerenchyma formation and formation of a ROL barrier
449 in roots (cf. Armstrong 1979).

450 Suberin and lignin have been proposed as components of the root ROL barrier
451 (reviewed by Watanabe *et al.* 2013), with circumstantial evidence for involvement of
452 suberin but not lignin in roots of rice (cv. Nipponbare) (Shiono *et al.* 2014b). Our
453 finding that the suberin accumulation pattern in roots, as visualized by use of a

454 histochemical stain, of line #468 (which forms a tight ROL barrier) was similar to the
455 patterns of maize (Fig. 5) suggests that the locus/loci located on chromosome 3 does not
456 affect the pattern of suberin accumulation as assessed using Fluorol Yellow 088. Suberin
457 contains polymers that are made up of various monomers and that have higher-order
458 structure (Bernards 2002; Franke & Schreiber 2007; Graça & Santos 2007). Mutation of
459 the rice *RCN1/OsABCG5* gene, which is involved in hypodermal/exodermal
460 suberization of roots, changed the suberin monomer composition and increased the
461 permeability to solutes in the root hypodermis/exodermis of rice plants grown under
462 stagnant deoxygenated conditions (Shiono *et al.* 2014a). Moreover, the composition of
463 suberin monomers in the outer parts of rice roots are different between plants in aerated
464 and stagnant deoxygenated conditions (Kotula *et al.* 2009a; Ranathunge *et al.* 2011).
465 Thus, the permeability of suberin lamellae to oxygen and solutes might depend on the
466 suberin monomer composition and/or the structure, analysis of which requires more
467 sophisticated approaches than histochemical staining. *Z. nicaraguensis* and maize roots
468 form suberin lamellae at the hypodermis/exodermis under stagnant deoxygenated
469 conditions (Fig. 5). However, maize roots are much more permeable to oxygen (Fig. 1)
470 as well as apoplastic solutes (periodic acid) as compared with *Z. nicaraguensis* roots
471 (Fig. 7). It would be of interest to determine whether there are differences in suberin
472 monomer composition or the arrangement of suberin deposition within cell walls
473 between *Z. nicaraguensis* and maize roots.

474 We previously found that some hypodermal/exodermal cells in adventitious roots
475 of maize grown under stagnant deoxygenated conditions lacked suberin lamellae (Abiko
476 *et al.* 2012). However, in this present study, passage cells lacking suberin lamellae were
477 not observed at the hypodermis/exodermis of maize roots under stagnant deoxygenated

478 condition (Fig. 5), but ROL amounts were still high from basal parts of maize roots (Fig.
479 1), suggesting that the passage cells lacking suberin lamellae cannot explain differences
480 in root ROL between maize and *Z. nicaraguensis*. During the growth of roots, cell walls
481 of the passage cells in the endodermis or hypodermis/exodermis are eventually
482 suberized to form suberin lamellae (Enstone *et al.* 2003). Thus, the presence or absence
483 of passage cells lacking suberin lamellae may depend on the age of the plants or roots,
484 or on when the stagnant solution treatments were imposed, but clearly these suberin
485 lamellae alone are not the tight barrier to ROL.

486 Some studies have suggested that lignin is a component of the ROL barrier in rice
487 (cv. Azucena) (Kotula *et al.* 2009a; Ranathunge *et al.* 2011), but this may not be the
488 case in another rice cultivar (Nipponbare) (Shiono *et al.* 2011, 2014b) or indeed in some
489 other wetland plants (De Simone *et al.* 2003; Soukup *et al.* 2007). Our finding of lignin
490 in the roots of *Z. nicaraguensis* but not in the roots of line #468 (Fig. 6), both of which
491 formed a tight ROL barrier (Figs. 1B & 4), indicates that lignin accumulation is not
492 involved in root ROL barrier formation in line #468.

493 Suberin and lignin have been suggested to be components of an apoplastic barrier
494 to the entry of toxic compounds (phytotoxins) in reduced soils (Enstone *et al.* 2003).
495 The root ROL barrier was previously hypothesized to not only impede ROL but also
496 restrict phytotoxin ingress (Armstrong 1979), and as demonstrated in a few studies (e.g.
497 Armstrong & Armstrong 2005). It should be noted that the apparent resistance to
498 oxygen of the barrier to ROL includes oxygen consumption across the
499 hypodermis/exodermis (Garthwaite *et al.* 2008; Kotula *et al.* 2009b), whereas in the
500 case of the apoplastic solute tracer this is not ‘consumed’ by the cells. Although it is
501 unclear whether an apoplastic barrier to solutes is the same as the ROL barrier, the two

502 barriers seem to coincide in position both radially and axially, i.e. at the outer tangential
503 and radial walls of the hypodermis/exodermis. Roots of line #468 contained an
504 apoplastic barrier to solutes (periodic acid) (Fig. 7) and exhibited a barrier to ROL (Figs.
505 3B & 4), but unlike *Z. nicaraguensis*, line #468 did not show prominent suberin and
506 lignin components in the outer cell layers (Figs. 5 & 6) so the barrier(s) are apparently
507 due to subtle changes (i.e. not distinguishable by the histochemical stains). For example,
508 electron-dense materials were observed between the hypodermis/exodermis and
509 epidermis of rice roots and these coincided with the timing of ROL barrier induction,
510 which was before histochemical changes in suberin could be detected (Shiono *et al.*
511 2011). Such changes in cell wall materials might be important for both the ROL barrier
512 and the observed changes in solute permeability in the outer parts of the roots.

513 Before line #468 can be used for maize breeding programs, undesirable *Z.*
514 *nicaraguensis* fragments on chromosomes 3, 9 and 10 (Fig. 3A) need to be removed
515 through backcrossing. Then, it should be possible to create a near isogenic line (NIL)
516 possessing the gene(s) controlling ROL barrier formation in the genetic background of
517 maize inbred line Mi29. The NIL for the root ROL barrier could be useful for the
518 development of waterlogging-tolerant F₁ cultivars, because maize inbred line Mi29 is
519 often used as a female parent of F₁ cultivars (Ikegaya *et al.* 1999a; Ito *et al.* 2004).
520 Moreover, the locus/loci for ROL barrier formation should be useful for improvement of
521 waterlogging tolerance of maize by several means, including QTL pyramiding this locus
522 (or loci) with other loci for above-ground adventitious root formation (Mano *et al.*
523 2009), constitutive aerenchyma formation (Mano *et al.* 2007) and tolerance under
524 reducing soil conditions (Mano & Omori 2013a).

525 In conclusion, we found that the short-arm of chromosome 3 in *Z. nicaraguensis* is

526 responsible for controlling formation of a tight ROL barrier in roots as well as reducing
527 permeability of the outer cell layers to apoplastic solute movement. Root ROL barrier
528 formation was associated with a ~22.6 Mb chromosomal region. We are currently
529 producing a NIL (near isogenic line) for future use in fine mapping of the locus (or loci)
530 for formation of the ROL and solute barrier(s) in the outer part of the roots, and with the
531 objective to clone the responsible gene(s). Cloning and functional analyses of these root
532 barrier-regulating gene(s) will elucidate the molecular mechanism of root ROL barrier
533 formation and the relationship of the barrier to ROL also with altered solute
534 permeability to restrict soil phytotoxin entry into roots.

535

536 **Acknowledgments**

537 We thank the International Maize and Wheat Improvement Center (CIMMYT) for
538 providing seeds of *Z. nicaraguensis* and Kyushu Okinawa Agricultural Research Center,
539 NARO for providing seeds of maize (inbred line Mi29). We thank Drs. Y. Sato, Y.
540 Inukai, T. Yamauchi, L. Schreiber, R. Franke and F. Waßmann for stimulating
541 discussions. This work was partly supported by a grant from “Development of
542 mitigation and adaptation techniques to global warming in the sectors of agriculture,
543 forestry, and fisheries” (4203) to YM and by the Japan Society for the Promotion of
544 Science (JSPS) KAKENHI Grant (15H04434) to MN. KW was supported by a
545 fellowship for doctoral course students from JSPS.

546 **References**

547

548 **Abiko T., Kotula L., Shiono K., Malik A.I., Colmer T.D. & Nakazono M. (2012)**

549 Enhanced formation of aerenchyma and induction of a barrier to radial oxygen loss
550 in adventitious roots of *Zea nicaraguensis* contribute to its waterlogging tolerance as
551 compared with maize (*Zea mays* ssp. *mays*). *Plant, Cell and Environment* 35,
552 1618–1630.

553 **Armstrong J. & Armstrong W. (1988)** *Phragmites australis* – A preliminary study of

554 soil-oxidizing sites and internal gas transport pathways. *New Phytologist* 108,
555 373–382.

556 **Armstrong J. & Armstrong W. (2005)** Rice: Sulfide-induced barriers to root radial

557 oxygen loss, Fe²⁺ and water uptake, and lateral root emergence. *Annals of Botany* 96,
558 625–638.

559 **Armstrong J., Armstrong W. & Beckett P.M. (1992)** *Phragmites australis*: Venturi-

560 and humidity-induced pressure flows enhance rhizome aeration and rhizosphere
561 oxidation. *New Phytologist* 120, 197–207.

562 **Armstrong W. (1979)** Aeration in higher plants. *Advances in Botanical Research* 7,

563 225–332.

564 **Armstrong W., Armstrong J. & Beckett P.M. (1990)** Measurement and modelling of

565 oxygen release from roots of *Phragmites australis*. In *The Use of Constructed*
566 *Wetlands in Water Pollution Control* (eds P. Cooper & B. C. Finklatter), pp. 41–54.
567 Pergamon Press, Oxford, UK.

568 **Armstrong W., Brändle R. & Jackson M.B. (1994)** Mechanisms of flood tolerance in

569 plants. *Acta Botanica Neerlandica* 43, 307–358.

- 570 **Armstrong W., Cousins D., Armstrong J., Turner D.W. & Beckett P.M. (2000)**
571 Oxygen distribution in wetland plant roots and permeability barriers to
572 gas-exchange with the rhizosphere: a microelectrode and modelling study with
573 *Phragmites australis*. *Annals of Botany* 86, 687–703.
- 574 **Armstrong W., Healy M.T. & Lythe S. (1983)** Oxygen diffusion in pea II. Oxygen
575 concentration in the primary root apex as affected by growth, the production of
576 laterals and radial oxygen loss. *New Phytologist* 94, 549–559.
- 577 **Armstrong W. & Wright E.J. (1975)** Radial oxygen loss from roots: the theoretical
578 basis for the manipulation of flux data obtained by the cylindrical platinum
579 electrode technique. *Physiologia Plantarum* 35, 21–26.
- 580 **Bailey-Serres J., Lee S.C. & Brinton E. (2012)** Waterproofing crops: Effective
581 flooding survival strategies. *Plant Physiology* 160, 1698–1709.
- 582 **Bernards M.A. (2002)** Demystifying suberin. *Canadian Journal of Botany* 80,
583 227–240
- 584 **Brundrett M.C., Kendrick B. & Peterson C.A. (1991)** Efficient lipid staining in plant
585 material with sudan red 7B or fluoral yellow 088 in polyethylene glycol-glycerol.
586 *Biotechnic and Histochemistry* 66, 111–116.
- 587 **Chandrasekaran S. & Yoshida T. (1973)** Effect of organic acid transformations in
588 submerged soils on growth of the rice plant. *Soil Science and Plant Nutrition* 19,
589 39–45.
- 590 **Colmer T.D. (2003a)** Aerenchyma and an inducible barrier to radial oxygen loss
591 facilitate root aeration in upland, paddy and deep-water rice (*Oryza sativa* L.).
592 *Annals of Botany* 91, 301–309.

593 **Colmer T.D. (2003b)** Long-distance transport of gases in plants: a perspective on
594 internal aeration and radial oxygen loss from roots. *Plant, Cell and Environment* 26,
595 17–36.

596 **Colmer T.D., Cox M.C.H. & Voesenek L.A.C.J. (2006)** Root aeration in rice (*Oryza*
597 *sativa*): evaluation of oxygen, carbon dioxide, and ethylene as possible regulators of
598 root acclimatizations. *New Phytologist* 170, 767–778.

599 **Colmer T.D., Gibberd M.R., Wiengweera A. & Tinh T.K. (1998)** The barrier to
600 radial oxygen loss from roots of rice (*Oryza sativa* L.) is induced by growth in
601 stagnant solution. *Journal of Experimental Botany* 49, 1431–1436.

602 **Colmer T.D. & Voesenek L.A.C.J. (2009)** Flooding tolerance: suites of plant traits in
603 variable environments. *Functional Plant Biology* 36, 665–681.

604 **De Simone O., Haase K., Müller E., Junk W.J., Hartmann K., Schreiber L. &**
605 **Schmidt W. (2003)** Apoplasmic barriers and oxygen transport properties of
606 hypodermal cell walls in roots from four Amazonian tree species. *Plant Physiology*
607 132, 206–217.

608 **Enstone D.E., Peterson C.A. & Ma F. (2003)** Root endodermis and exodermis:
609 structure, function, and responses to the environment. *Journal of Plant Growth*
610 *Regulation* 21, 335–351.

611 **Franke R. & Schreiber L. (2007)** Suberin - a biopolyester forming apoplastic plant
612 interfaces. *Current Opinion in Plant Biology* 10, 252–259.

613 **Garthwaite A.J., Armstrong W. & Colmer TD. (2008)** Assessment of O₂ diffusivity
614 across the barrier to radial O₂ loss in adventitious roots of *Hordeum marinum*. *New*
615 *Phytologist* 179, 405–416.

- 616 **Graça J. & Santos S. (2007)** Suberin: a biopolyester of plants' skin. *Macromolecular*
617 *Bioscience* 7, 128–135.
- 618 **Ikegaya F., Koinuma K. & Ito E. (1999a)** Development and characteristics of new
619 silage maize cultivar "Yumesodachi". *Bulletin of the Kyushu National Agricultural*
620 *Experiment Station* 35, 49–69. (In Japanese with English summary)
- 621 **Ikegaya F., Koinuma K., Ito E., Inoue Y., Nozaki K., Fujita K. & Mochizuki N.**
622 **(1999b)** Development and characteristics of new inbred line "Mi29" for silage
623 maize. *Bulletin of the Kyushu National Agricultural Experiment Station* 35, 71–83.
624 (In Japanese with English summary)
- 625 **Iltis H.H. & Benz B.F. (2000)** *Zea nicaraguensis* (Poaceae), a new teosinte from
626 pacific coastal Nicaragua. *Novon* 10, 382–390.
- 627 **Ito E., Ikegaya F., Koinuma K. & Eguchi K. (2004)** Development and characteristics
628 of new silage maize cultivar "Yumechikara". *Bulletin of the Kyushu National*
629 *Agricultural Experiment Station* 43, 1–24. (in Japanese with English summary)
- 630 **Jensen W.A. (1962)** *Botanical Histochemistry*. N. H. Freeman & Company, San
631 Francisco, CA, USA.
- 632 **Justin S.H.F.W. & Armstrong W. (1987)** The anatomical characteristics of roots and
633 plant response to soil flooding. *New Phytologist* 106, 465–495.
- 634 **Kirk G.J.D., Greenway H., Atwell B.J., Ismail A.M. & Colmer T.D. (2014)**
635 Adaptation of rice to flooded soils. *Progress in Botany* 75, 215–253.
- 636 **Kotula L., Ranathunge K., Schreiber L. & Steudle E. (2009a)** Functional and
637 chemical comparison of apoplastic barriers to radial oxygen loss in roots of rice
638 (*Oryza sativa* L.) grown in aerated or deoxygenated solution. *Journal of*
639 *Experimental Botany* 60, 2155–2167.

640 **Kotula L., Ranathunge K. & Steudle E. (2009b)** Apoplastic barriers effectively block
641 oxygen permeability across outer cell layers of rice roots under deoxygenated
642 conditions: roles of apoplastic pores and of respiration. *New Phytologist* 184,
643 909–917.

644 **Kotula L. & Steudle E. (2009)** Measurements of oxygen permeability coefficients of
645 rice (*Oryza sativa* L.) roots using a new perfusion technique. *Journal of*
646 *Experimental Botany* 60, 567–580.

647 **Kulichikhin K., Yamauchi T., Watanabe K. & Nakazono M. (2014)** Biochemical and
648 molecular characterization of rice (*Oryza sativa* L.) roots forming a barrier to radial
649 oxygen loss. *Plant, Cell and Environment* 37, 2406–2420.

650 **Lux A., Morita S., Abe J. & Ito K. (2005)** An improved method for clearing and
651 staining free-hand sections and whole-mount samples. *Annals of Botany* 96,
652 989–996.

653 **Mae T. & Ohira K. (1981)** The remobilization of nitrogen related to leaf growth and
654 senescence in rice plants (*Oryza sativa* L.). *Plant & Cell Physiology* 22, 1067–1074.

655 **Malik A.I., Islam A.K.M.R. & Colmer T.D. (2011)** Transfer of the barrier to radial
656 oxygen loss in roots of *Hordeum marinum* to wheat (*Triticum aestivum*): evaluation
657 of four *H. marinum*–wheat amphiploids. *New Phytologist* 190, 499–508.

658 **Mano Y. & Omori F. (2007)** Breeding for flooding tolerant maize using “teosinte” as a
659 germplasm resource. *Plant Root* 1, 17–21.

660 **Mano Y. & Omori F. (2008)** Verification of QTL controlling root aerenchyma
661 formation in a maize × teosinte “*Zea nicaraguensis*” advanced backcross population.
662 *Breeding Science* 58, 217–223.

663 **Mano Y. & Omori F. (2009)** High-density linkage map around the root aerenchyma
664 locus *Qaer1.06* in the backcross populations of maize Mi29 × teosinte “*Zea*
665 *nicaraguensis*”. *Breeding Science* 59, 427–433.

666 **Mano Y. & Omori F. (2013a)** Flooding tolerance in interspecific introgression lines
667 containing chromosome segments from teosinte (*Zea nicaraguensis*) in maize (*Zea*
668 *mays subsp. mays*). *Annals of Botany* 112, 1125–1139.

669 **Mano Y. & Omori F. (2013b)** Relationship between constitutive root aerenchyma
670 formation and flooding tolerance in *Zea nicaraguensis*. *Plant and Soil* 370,
671 447–460.

672 **Mano Y., Omori F., Loaisiga C.H. & Bird R.M. (2009)** QTL mapping of
673 above-ground adventitious roots during flooding in maize x teosinte “*Zea*
674 *nicaraguensis*” backcross population. *Plant Root* 3, 3–9.

675 **Mano Y., Omori F., Takamizo T., Kindiger B., Bird R.M., Loaisiga C.H. &**
676 **Takahashi H. (2007)** QTL mapping of root aerenchyma formation in seedlings of a
677 maize × rare teosinte “*Zea nicaraguensis*” cross. *Plant and Soil* 295, 103–113.

678 **Mano Y., Omori F., Tamaki H., Mitsuhashi S. & Takahashi W. (2016)** DNA
679 marker-assisted selection approach for developing flooding-tolerant maize. *The*
680 *Japan Agricultural Research Quarterly* 50, 175–182.

681 **Naredo M.E.B., Juliano A.B., Lu B.R., De Guzman F. & Jackson M.T. (1998)**
682 Responses to seed dormancy-breaking treatments in rice species (*Oryza* L.). *Seed*
683 *Science and Technology* 26, 675–689.

684 **Pecková E., Tylová E. & Soukup A. (2016)** Tracing root permeability: comparison of
685 tracer methods. *Biologia Plantarum*, in press.

686 **Ranathunge K., Lin J., Steudle E. & Schreiber L. (2011)** Stagnant deoxygenated
687 growth enhances root suberization and lignifications, but differentially affects water
688 and NaCl permeabilities in rice (*Oryza sativa* L.) roots. *Plant, Cell and Environment*
689 34, 1223–1240.

690 **Raskin I. (1983)** A method for measuring leaf volume, density, thickness, and internal
691 gas volume. *HortScience* 18, 698–699.

692 **Shiono K., Ando M., Nishiuchi S., Takahashi H., Watanabe K., Nakamura M., ...,**
693 **Kato K. (2014a)** RCN1/OsABCG5, an ATP-binding cassette (ABC) transporter, is
694 required for hypodermal suberization of roots in rice (*Oryza sativa*). *The Plant*
695 *Journal* 80, 40–51.

696 **Shiono K., Ogawa S., Yamazaki S., Isoda H., Fujimura T., Nakazono M. & Colmer**
697 **T.D. (2011)** Contrasting dynamics of radial O₂-loss barrier induction and
698 aerenchyma formation in rice roots of two lengths. *Annals of Botany* 107, 89–99.

699 **Shiono K., Yamauchi T., Yamazaki S., Mohanty B., Malik A.I., Nagamura Y., ...,**
700 **Nakazono M. (2014b)** Microarray analysis of laser-microdissected tissues indicates
701 the biosynthesis of suberin in the outer part of roots during formation of a barrier to
702 radial oxygen loss in rice (*Oryza sativa*). *Journal of Experimental Botany* 65,
703 4795–4806.

704 **Sorrell B.K., Mendelsohn I.A., McKee K.L. & Woods R.A. (2000).** Ecophysiology
705 of wetland plant roots: a modelling comparison of aeration in relation to species
706 distribution. *Annals of Botany* 86, 675–685.

707 **Soukup A., Armstrong W., Schreiber L., Franke R. & Votrubová O. (2007)**
708 Apoplastic barriers to radial oxygen loss and solute penetration: a chemical and

709 functional comparison of the exodermis of two wetland species, *Phragmites*
710 *australis* and *Glyceria maxima*. *New Phytologist* 173, 264–278.

711 **Thomson C.J., Armstrong W., Waters I. & Greenway H. (1990)** Aerenchyma
712 formation and associated oxygen movement in seminal and nodal roots of wheat.
713 *Plant, Cell and Environment* 13, 395–403.

714 **Voesenek L.A.C.J. & Bailey-Serres J. (2015)** Flood adaptive traits and processes: an
715 overview. *New Phytologist* 206, 57–73.

716 **Watanabe K., Nishiuchi S., Kulichikhin K. & Nakazono M. (2013)** Does suberin
717 accumulation in plant roots contribute to waterlogging tolerance? *Frontiers in Plant*
718 *Science* 4, 178.

719 **Wiengweera A., Greenway H. & Thomson C.J. (1997)** The use of agar nutrient
720 solution to simulate lack of convection in waterlogged soils. *Annals of Botany* 80,
721 115–123.

722

723 **Supporting information**

724

725 **Figure S1.** Chromosome structure of introgression line (IL) series. Black and white
726 boxes indicate chromosome segments derived from *Z. nicaraguensis* and *Z. mays* ssp.
727 *mays* (maize), respectively. Grey boxes indicate heterozygous regions. Genotypes of
728 some ILs were somewhat different to the original ILs reported by Mano & Omori
729 (2013a), because we used the sister lines in cases where seed numbers of the original
730 ILs were limited.

731

732 **Figure S2.** Whole root porosity (% , gas volume per unit root volume) of *Z.*
733 *nicaraguensis*, *Z. mays* ssp. *mays* (maize), and introgression lines (ILs; *Z. nicaraguensis*
734 chromosome segments in *Z. mays* ssp. *mays*) IL#11, #468 and IL#42. Plants were raised
735 for 11 days and then grown for 2 weeks in stagnant deoxygenated solution. Values are
736 means (n = 4) \pm SD. * indicates significant difference compared to *Z. nicaraguensis* (p
737 < 0.1, one-way ANOVA and then Dunnett's test).

738

739 **Figure S3.** Evaluation of abilities of ROL barrier formation in adventitious roots of
740 introgression line IL#11 plants possessing *Z. nicaraguensis*-derived chromosome 3
741 segment with homozygotes or heterozygotes or possessing the equivalent maize-derived
742 chromosome segment by a methylene blue staining assay. Plants were raised for 11
743 days and then grown for 2 weeks in stagnant deoxygenated solution. Shoots were in air
744 and roots were in an oxygen-free medium; blue indicates oxygen that has diffused
745 outwards from within the roots. Bar = 1 cm.

746

747 **Figure legends**

748

749 **Figure 1.** Evaluation of radial oxygen loss (ROL) barrier formation ability in
750 adventitious roots of *Z. mays* ssp. *mays* (maize) and *Z. nicaraguensis* by methylene blue
751 staining (A) and root-sleeving oxygen electrode (B). Maize and *Z. nicaraguensis* plants
752 were raised for 11 days and then grown for 2 weeks in stagnant deoxygenated solution.
753 (A) For the methylene blue staining assay, 4 independent plants of maize and *Z.*
754 *nicaraguensis* were used and each species showed similar results among 4 plants. Blue
755 indicates oxygen. Bar = 1 cm. The adventitious roots (lengths of 90 mm or greater) were
756 stained at room temperature (~25°C) under white light. (B) For ROL measurements by
757 the root-sleeving oxygen electrode, values are means ($n = 4$) \pm SD. The ROL of
758 adventitious roots (a length of 90 mm or greater) was measured at 28°C in a growth
759 chamber, with shoots in air and roots in an oxygen-free medium.

760

761 **Figure 2.** Evaluation of radial oxygen loss (ROL) barrier formation ability in
762 adventitious roots of 42 introgression lines (ILs; *Z. nicaraguensis* chromosome
763 segments in *Z. mays* ssp. *mays*) by a methylene blue staining assay. Plants were raised
764 for 11 days and then grown for 2 weeks in stagnant deoxygenated solution. For each
765 plant, an intact adventitious root was assessed. The adventitious roots of ILs (lengths of
766 60 mm or greater), except for IL#6 (ave. 59 mm) and IL#35 (ave. 48 mm), were stained
767 at room temperature (~25°C) under white light. Three or four independent plants were
768 used and each of the ILs showed similar results among 3 or 4 plants. Shoots were in air
769 and roots were in an oxygen-free medium; blue indicates oxygen that has diffused
770 outwards from within the roots. Bar = 1 cm.

771

772 **Figure 3.** Chromosome structure (A) and evaluation of root ROL barrier formation
773 abilities (B) of introgression lines (ILs; *Z. nicaraguensis* chromosome segments in *Z.*
774 *mays* ssp. *mays*) IL#11, #418, #422, #426, #468 and IL#42. (A) Black and white boxes
775 indicate chromosome segments derived from *Z. nicaraguensis* and *Z. mays* ssp. *mays*
776 (maize), respectively. Grey boxes indicate heterozygous regions. (B) Methylene blue
777 staining of an intact adventitious root each of maize, *Z. nicaraguensis* (*Z. nica.*) and
778 introgression lines IL#11, #418, #422, #426, #468 and IL#42. Four independent plants
779 of each line were used and each of them showed similar results among 4 plants. Shoots
780 were in air and roots were in an oxygen-free medium; blue indicates oxygen that has
781 diffused outwards from within the roots. The adventitious roots (lengths of 70 mm or
782 greater) were stained at room temperature (~25°C) under white light. Bar = 1 cm.

783

784 **Figure 4.** Radial oxygen loss (ROL) patterns along adventitious roots of introgression
785 lines (ILs; *Z. nicaraguensis* chromosome segments in *Z. mays* ssp. *mays*) IL#11, #418,
786 #422, #426, #468 and IL#42. ROL was measured using a root-sleeving oxygen
787 electrode. Shoots were in air and roots were in an oxygen-free medium. The ROL of
788 adventitious roots (lengths of 90 to 120 mm) were measured at 28°C in the growth
789 chamber. Values are means ($n = 4$) \pm SD.

790

791 **Figure 5.** Comparison of suberin lamellae development in the outer parts of roots of *Z.*
792 *mays* ssp. *mays* (maize), *Z. nicaraguensis*, and introgression lines (ILs; *Z. nicaraguensis*
793 chromosome segments in *Z. mays* ssp. *mays*) #468 and IL#42 grown in stagnant
794 deoxygenated solution. Cross-sections were made from 90-120 mm adventitious roots

795 of 26-day-old plants, stained with Fluorol yellow 088 and viewed under UV
796 illumination. The presence of suberin lamellae was detected by yellow-green
797 fluorescence. Bar = 50 μ m.

798

799 **Figure 6.** Comparison of lignin accumulation in the outer parts of roots of *Z. mays* ssp.
800 *mays* (maize), *Z. nicaraguensis*, and introgression lines (ILs; *Z. nicaraguensis*
801 chromosome segments in *Z. mays* ssp. *mays*) #468 and IL#42 grown in stagnant
802 deoxygenated solution. Cross-sections were made from 90-120 mm adventitious roots
803 of 26-day-old plants, stained with phloroglucinol-HCl and viewed under white light.
804 Lignin in cell walls was detected by red staining. Bar = 50 μ m.

805

806 **Figure 7.** Permeability of periodic acid in the outer parts of roots of *Z. mays* ssp. *mays*
807 (maize), *Z. nicaraguensis*, and introgression lines (ILs; *Z. nicaraguensis* chromosome
808 segments in *Z. mays* ssp. *mays*) #468 and IL#42 grown in stagnant deoxygenated
809 solution. Purple color indicates that the periodic acid penetrated into root tissues.
810 Cross-sections were made from 90-120 mm adventitious roots of 26-day-old plants,
811 stained with Schiff's staining and viewed under white light. Bar = 50 μ m.

812

813 **Figure 8.** Physical map of the chromosome 3 in introgression lines IL#5, IL#11 and
814 IL#12 [possessing *Z. nicaraguensis* chromosome segments in the genetic background of
815 *Z. mays* ssp. *mays* (maize)]. This map was made using 12 DNA makers [10 were used
816 for development of ILs (Mano & Omori 2013a) and the remaining 2 (umc2369,
817 umc1742) were newly added]. The positions of the DNA markers are determined by
818 BLAST (Basic Local Alignment Search Tool) analyses of the primer sequences in

819 MaizeGDB (<http://www.maizegdb.org/>). The locus (or loci) for ROL barrier formation
820 is mapped within a box with the dotted line. Black and white boxes indicate
821 chromosome segments derived from *Z. nicaraguensis* and *Z. mays* ssp. *mays* (maize),
822 respectively. Grey boxes indicate heterozygous regions of the chromosomes. In this
823 map, the recombined positions are tentatively shown in the middle of two neighbor
824 markers.

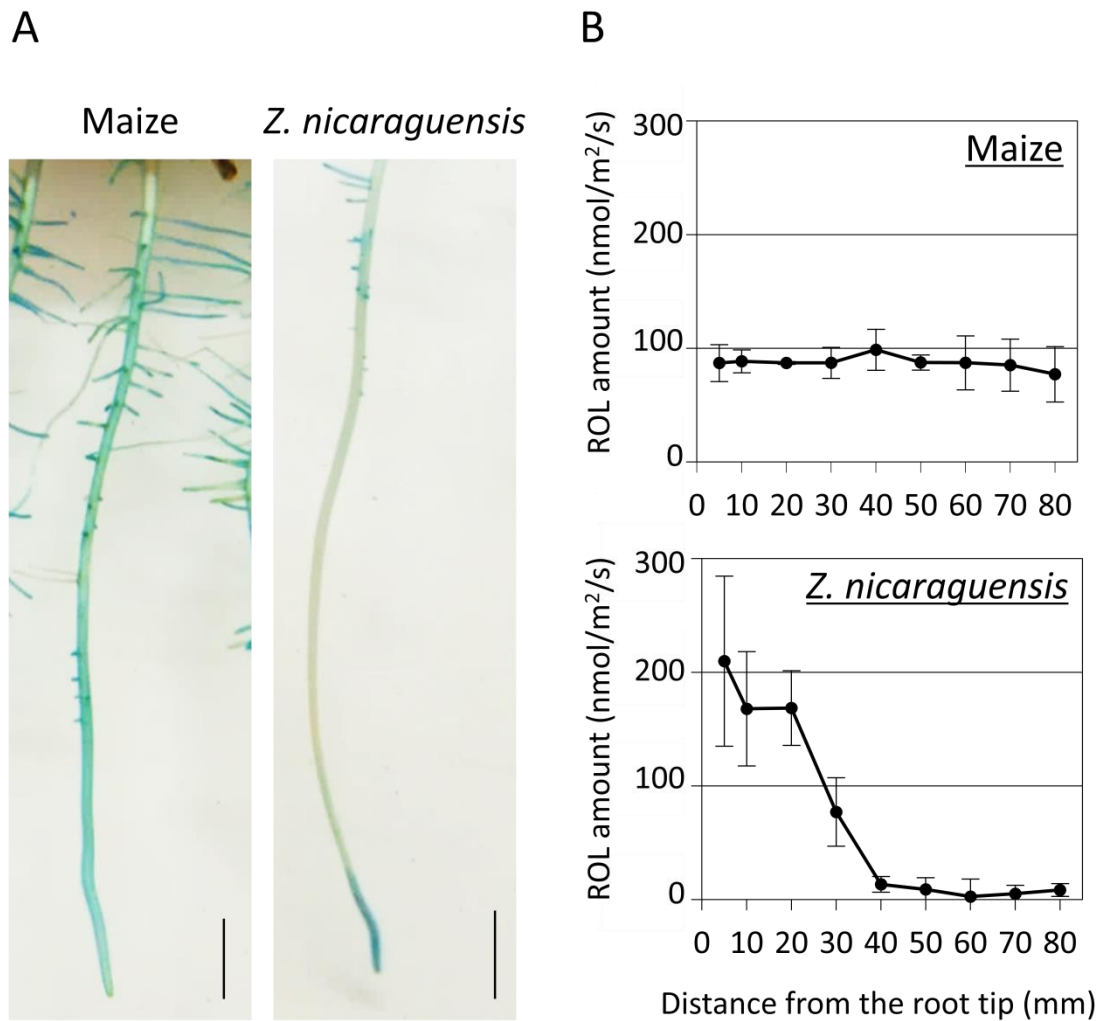


Figure 1. Evaluation of radial oxygen loss (ROL) barrier formation ability in adventitious roots of *Z. mays* ssp. *mays* (maize) and *Z. nicaraguensis* by methylene blue staining (A) and root-sleeving oxygen electrode (B). Maize and *Z. nicaraguensis* plants were raised for 11 days and then grown for 2 weeks in stagnant deoxygenated solution. (A) For the methylene blue staining assay, 4 independent plants of maize and *Z. nicaraguensis* were used and each species showed similar results among 4 plants. Blue indicates oxygen. Bar = 1 cm. The adventitious roots (lengths of 90 mm or greater) were stained at room temperature (~25°C) under white light. (B) For ROL measurements by the root-sleeving oxygen electrode, values are means ($n = 4$) \pm SD. The ROL of adventitious roots (a length of 90 mm or greater) was measured at 28°C in a growth chamber, with shoots in air and roots in an oxygen-free medium.

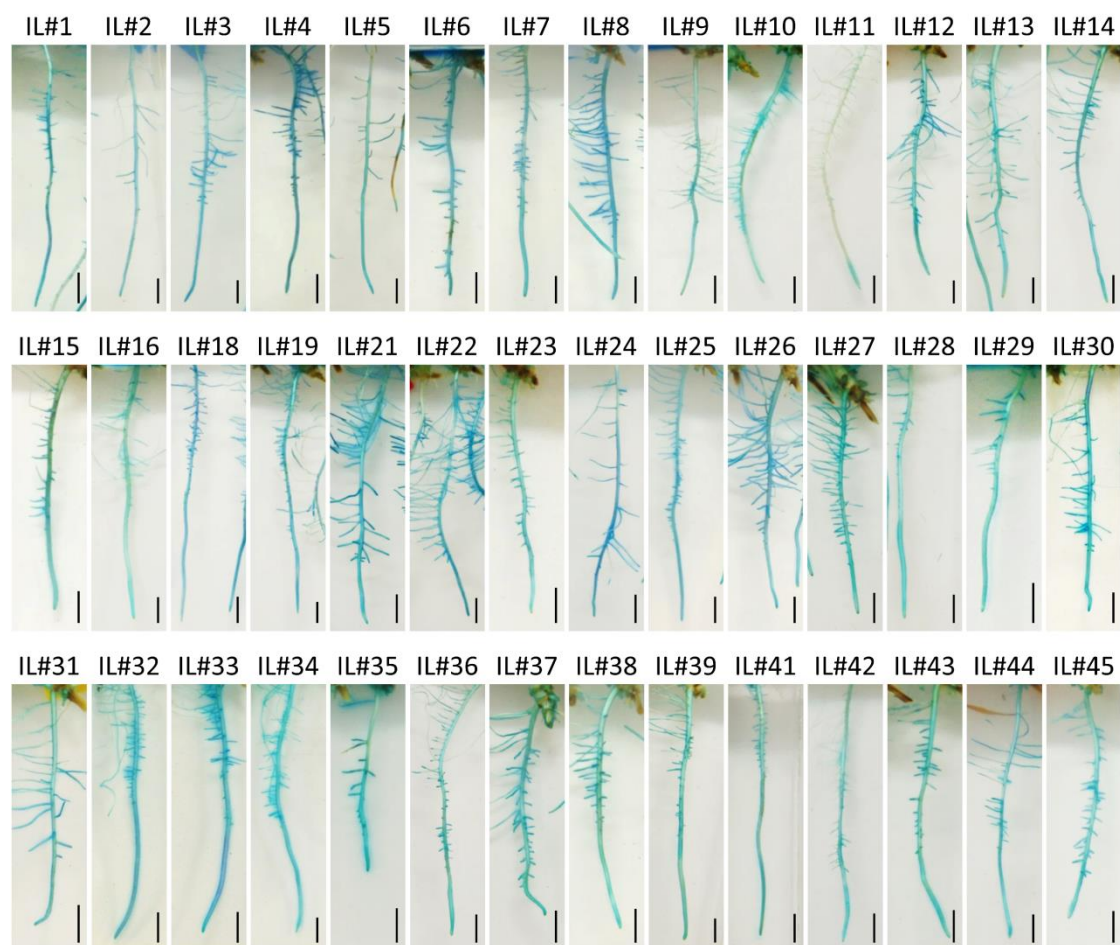


Figure 2. Evaluation of radial oxygen loss (ROL) barrier formation ability in adventitious roots of 42 introgression lines (ILs; *Z. nicaraguensis* chromosome segments in *Z. mays* ssp. *mays*) by a methylene blue staining assay. Plants were raised for 11 days and then grown for 2 weeks in stagnant deoxygenated solution. For each plant, an intact adventitious root was assessed. The adventitious roots of ILs (lengths of 60 mm or greater), except for IL#6 (ave. 59 mm) and IL#35 (ave. 48 mm), were stained at room temperature (~25°C) under white light. Three or four independent plants were used and each of the ILs showed similar results among 3 or 4 plants. Shoots were in air and roots were in an oxygen-free medium; blue indicates oxygen that has diffused outwards from within the roots. Bar = 1 cm.

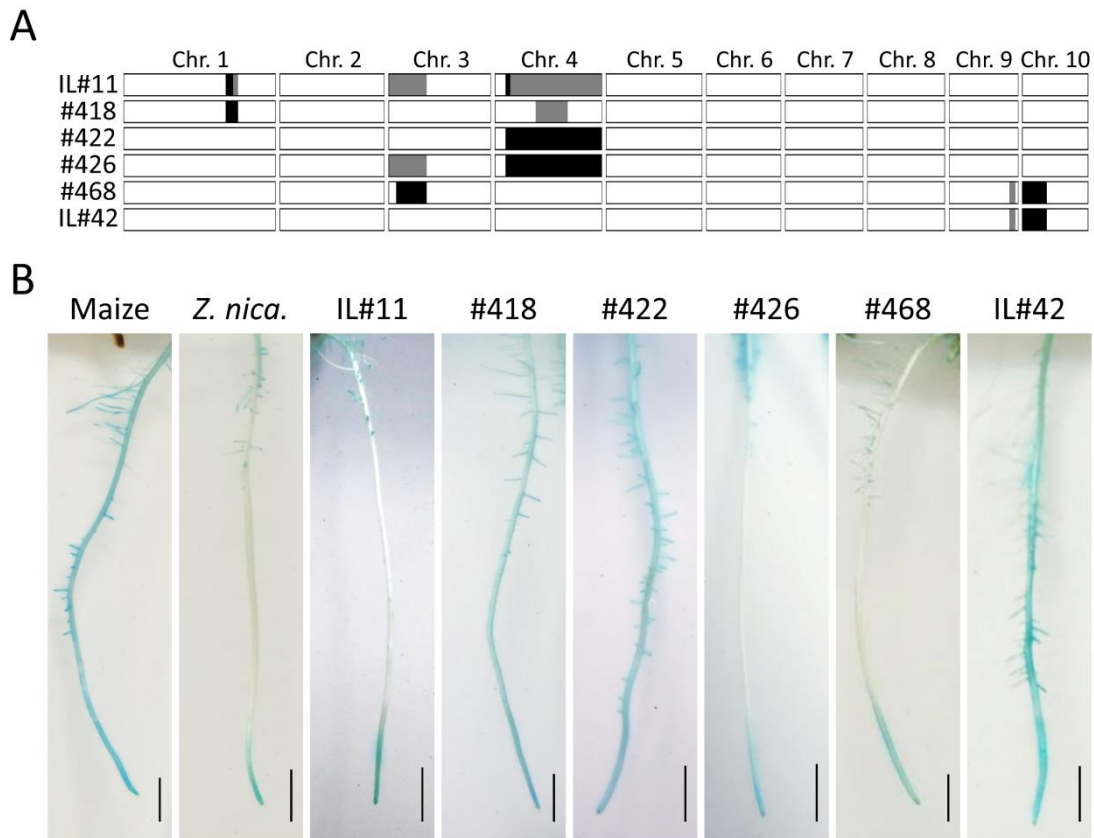


Figure 3. Chromosome structure (A) and evaluation of root ROL barrier formation abilities (B) of introgression lines (ILs; *Z. nicaraguensis* chromosome segments in *Z. mays* ssp. *mays*) IL#11, #418, #422, #426, #468 and IL#42. (A) Black and white boxes indicate chromosome segments derived from *Z. nicaraguensis* and *Z. mays* ssp. *mays* (maize), respectively. Grey boxes indicate heterozygous regions. (B) Methylene blue staining of an intact adventitious root each of maize, *Z. nicaraguensis* and introgression lines IL#11, #418, #422, #426, #468 and IL#42. Four independent plants of each line were used and each of them showed similar results among 4 plants. Shoots were in air and roots were in an oxygen-free medium; blue indicates oxygen that has diffused outwards from within the roots. The adventitious roots (lengths of 70 mm or greater) were stained at room temperature (~25°C) under white light. Bar = 1 cm.

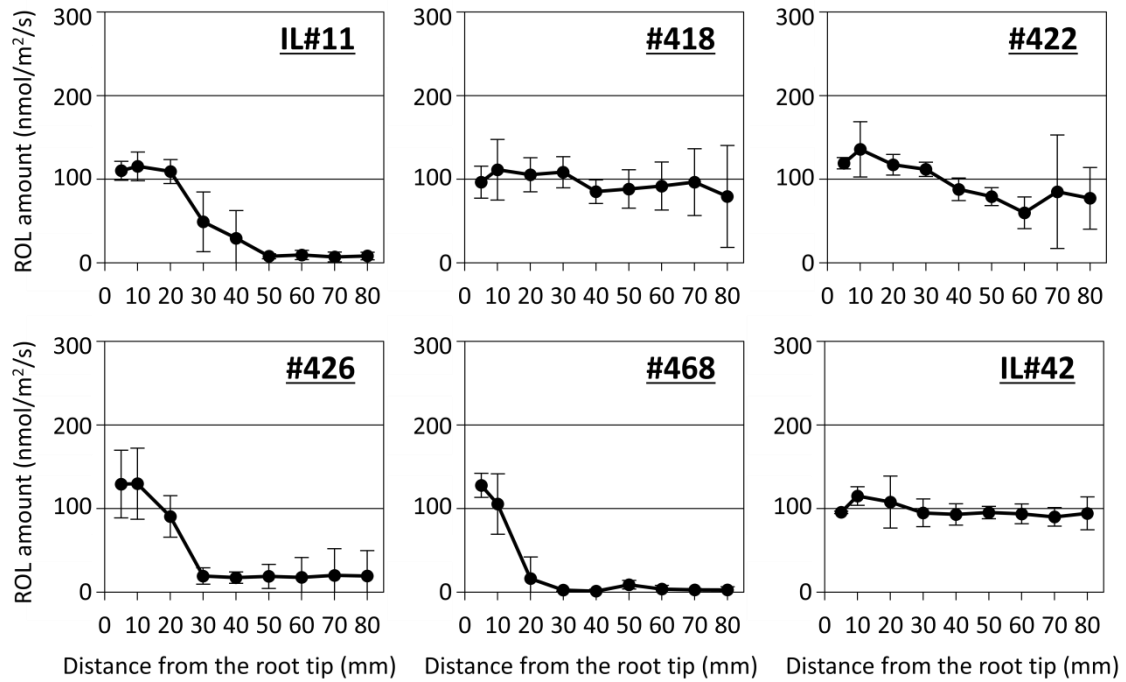


Figure 4. Radial oxygen loss (ROL) patterns along adventitious roots of introgression lines (ILs; *Z. nicaraguensis* chromosome segments in *Z. mays* ssp. *mays*) IL#11, #418, #422, #426, #468 and IL#42. ROL was measured using a root-sleeving oxygen electrode. Shoots were in air and roots were in an oxygen-free medium. The ROL of adventitious roots (lengths of 90 to 120 mm) were measured at 28°C in the growth chamber. Values are means ($n = 4$) \pm SD.

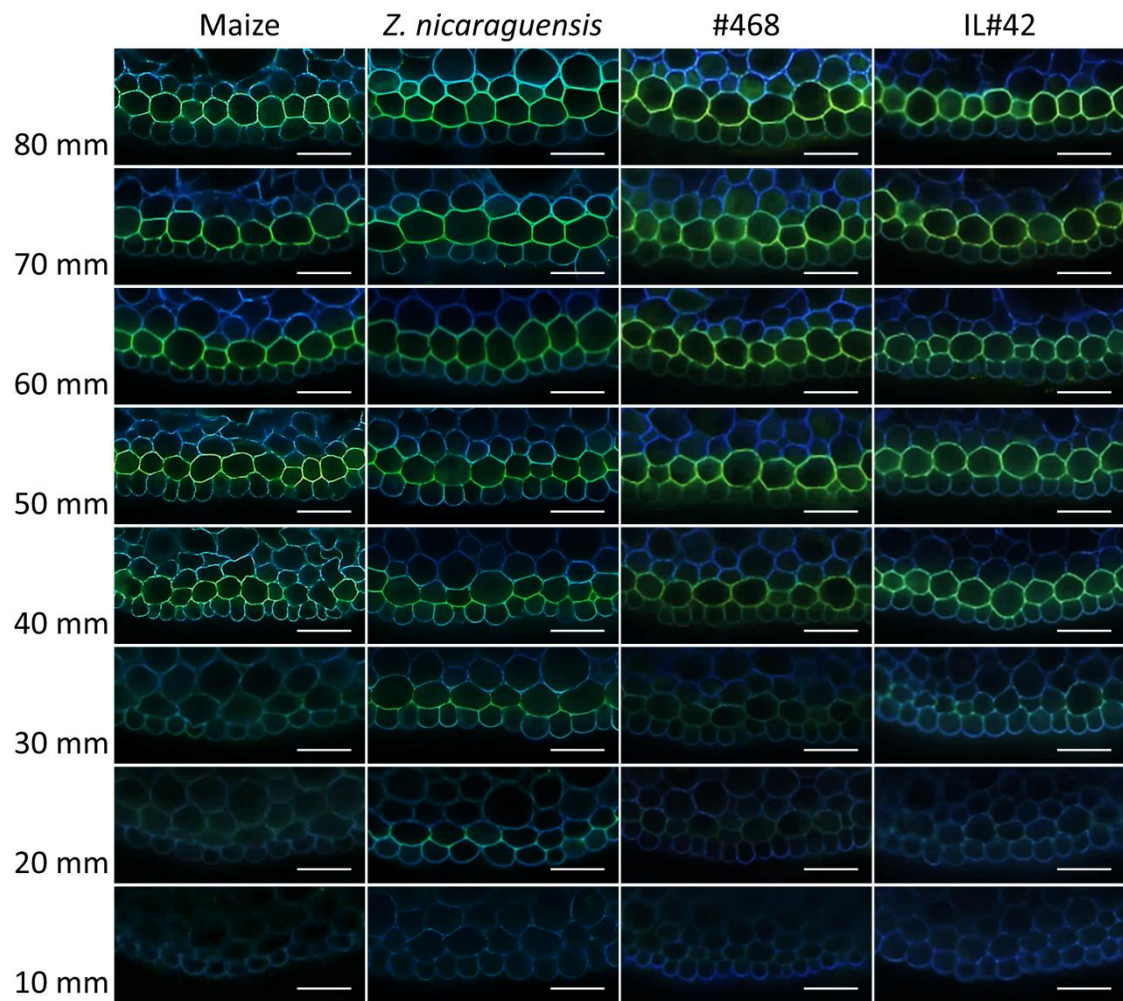


Figure 5. Comparison of suberin lamellae development in the outer parts of roots of *Z. mays* ssp. *mays* (maize), *Z. nicaraguensis*, and introgression lines (ILs; *Z. nicaraguensis* chromosome segments in *Z. mays* ssp. *mays*) #468 and IL#42 grown in stagnant deoxygenated solution. Cross-sections were made from 90-120 mm adventitious roots of 26-days-old plants, stained with Fluorol yellow 088 and viewed under UV illumination. The presence of suberin lamellae was detected by yellow-green fluorescence. Bar = 50 μ m.

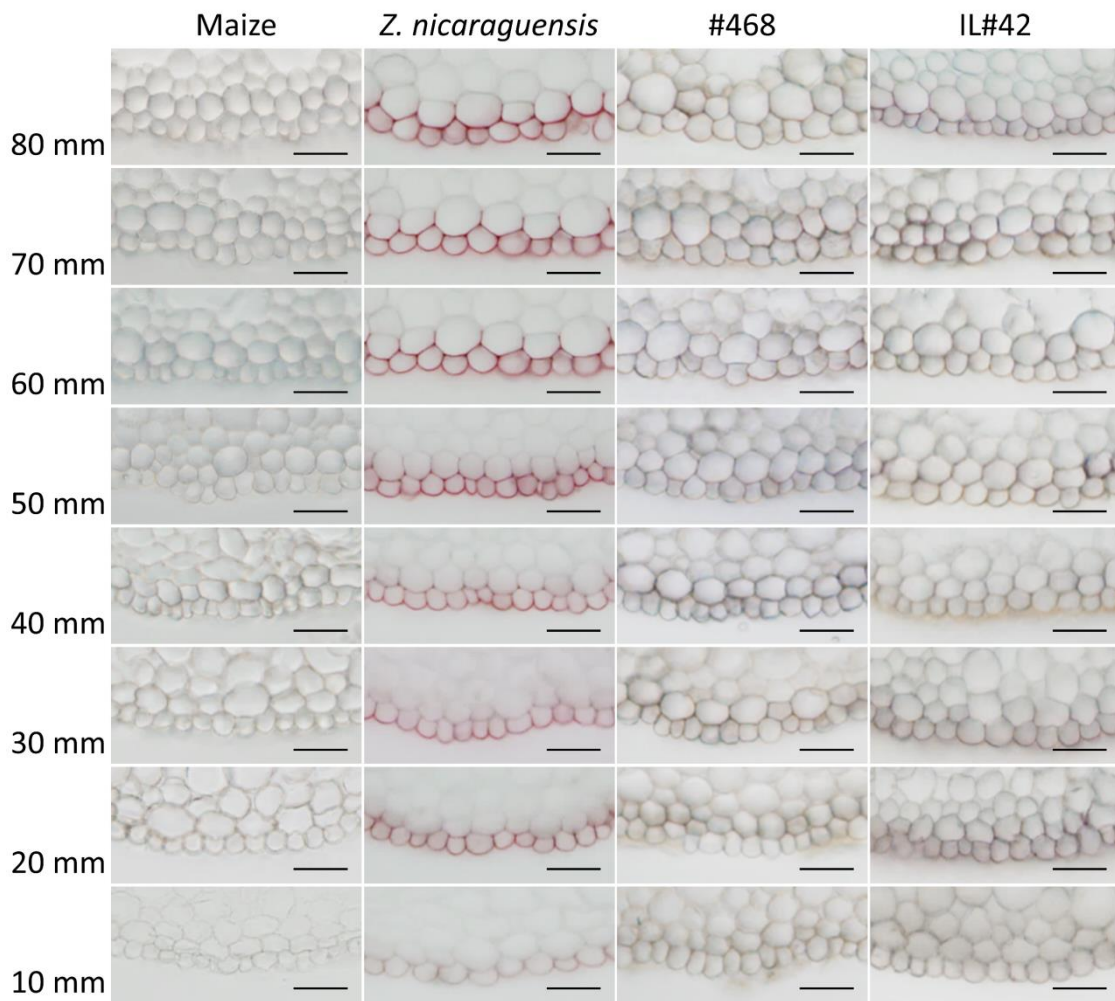


Figure 6. Comparison of lignin accumulation in the outer parts of roots of *Z. mays* ssp. *mays* (maize), *Z. nicaraguensis*, and introgression lines (ILs; *Z. nicaraguensis* chromosome segments in *Z. mays* ssp. *mays*) #468 and IL#42 grown in stagnant deoxygenated solution. Cross-sections were made from 90-120 mm adventitious roots of 26-days-old plants, stained with phloroglucinol-HCl and viewed under white light. Lignin in cell walls was detected by red staining. Bar = 50 μ m.

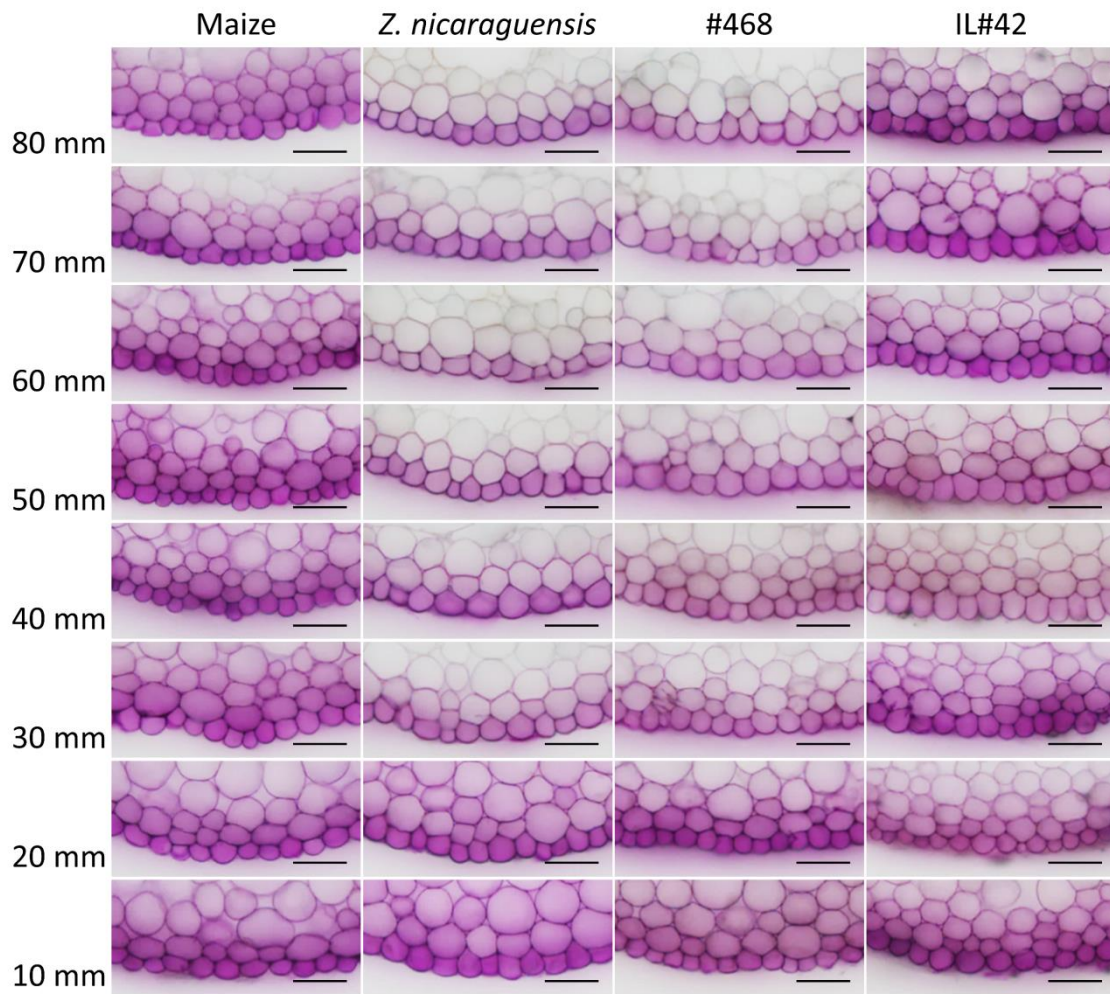


Figure 7. Permeability of periodic acid in the outer parts of roots of *Z. mays* ssp. *mays* (maize), *Z. nicaraguensis*, and introgression lines (ILs; *Z. nicaraguensis* chromosome segments in *Z. mays* ssp. *mays*) #468 and IL#42 grown in stagnant deoxygenated solution. Purple color indicates that the periodic acid penetrated into root tissues. Cross-sections were made from 90-120 mm adventitious roots of 26-days-old plants, stained with Schiff's staining and viewed under white light. Bar = 50 μ m.

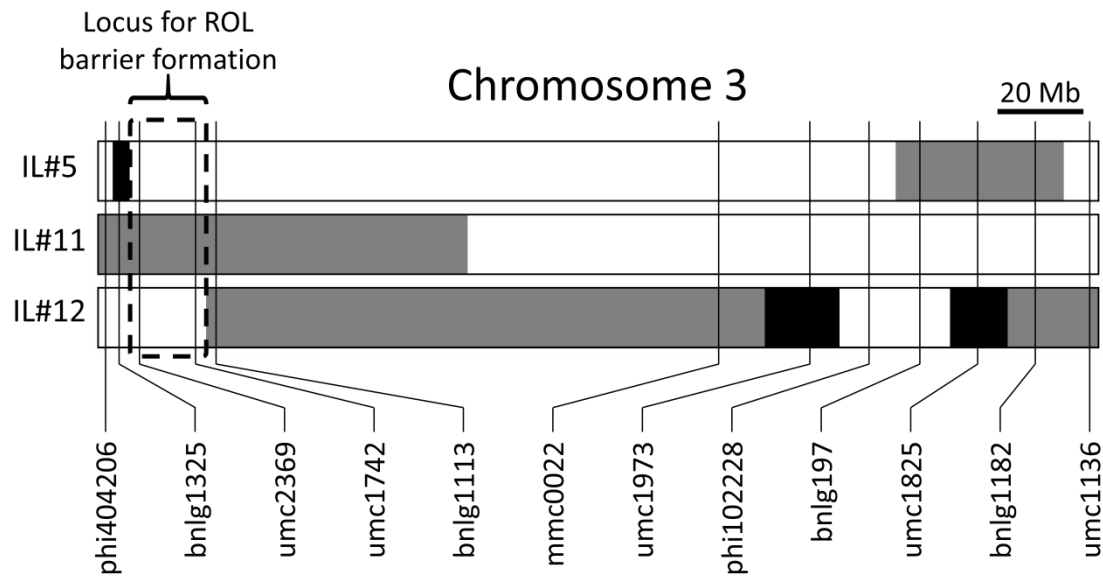


Figure 8. Physical map of the chromosome 3 in introgression lines IL#5, IL#11 and IL#12 [possessing *Z. nicaraguensis* chromosome segments in the genetic background of *Z. mays* ssp. *mays* (maize)]. This map was made using 12 DNA makers [10 were used for development of ILs (Mano & Omori 2013) and the remaining 2 (umc2369, umc1742) were newly added]. The positions of the DNA markers are determined by BLAST (Basic Local Alignment Search Tool) analyses of the primer sequences in MaizeGDB (<http://www.maizegdb.org/>). The locus (or loci) for ROL barrier formation is mapped within a box with the dotted line. Black and white boxes indicate chromosome segments derived from *Z. nicaraguensis* and *Z. mays* ssp. *mays* (maize), respectively. Grey boxes indicate heterozygous regions of the chromosomes. In this map, the recombined positions are tentatively shown in the middle of two neighbor markers.

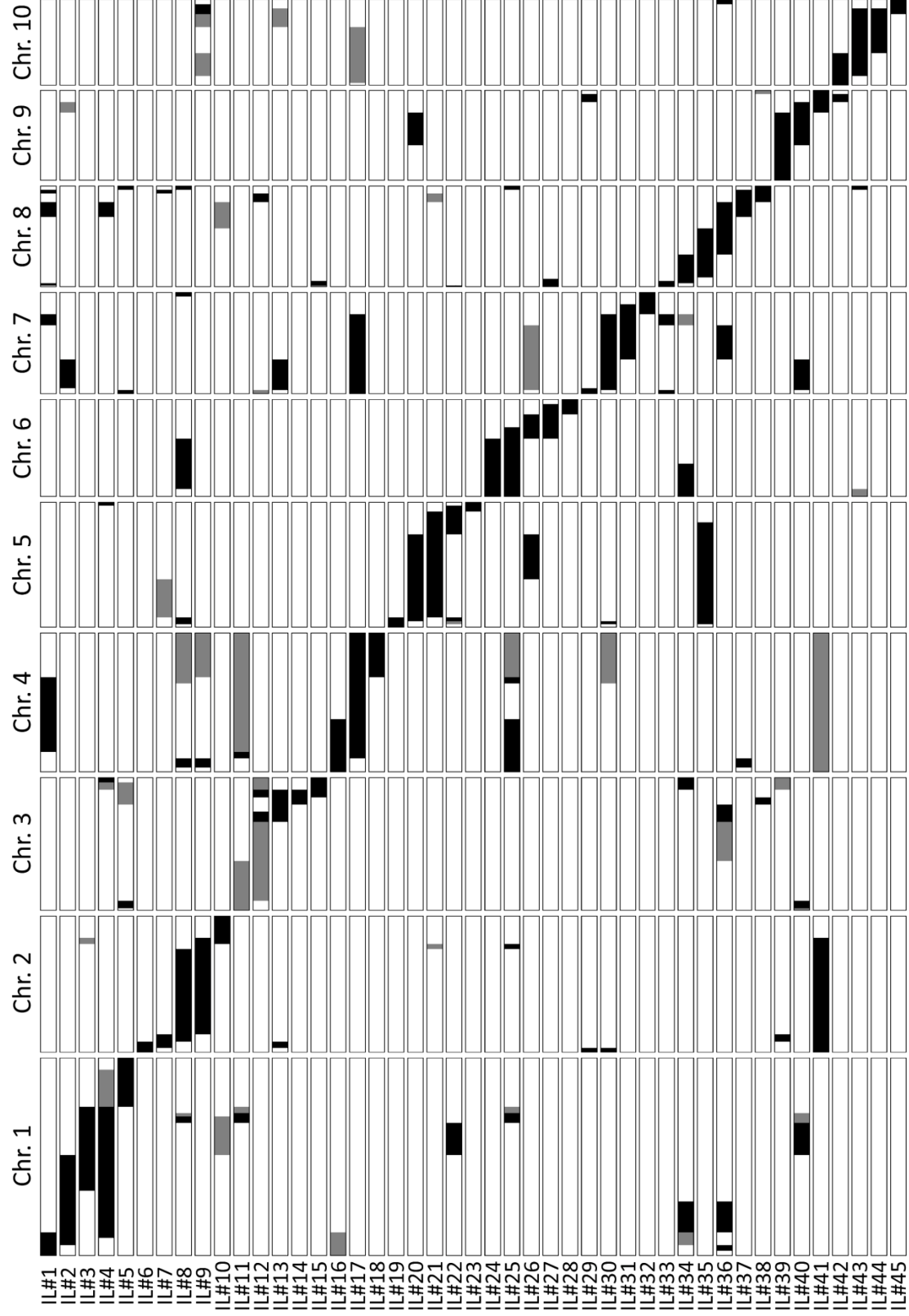


Figure S1. Chromosome structure of introgression line (IL) series. Black and white boxes indicate chromosome segments derived from *Z. nicaraguensis* and *Z. mays* ssp. *mays* (maize), respectively. Grey boxes indicate heterozygous regions. Genotypes of some ILs were somewhat different to the original ILs reported by Mano & Omori (2013a), because we used the sister lines in cases where seed numbers of the original ILs were limited.

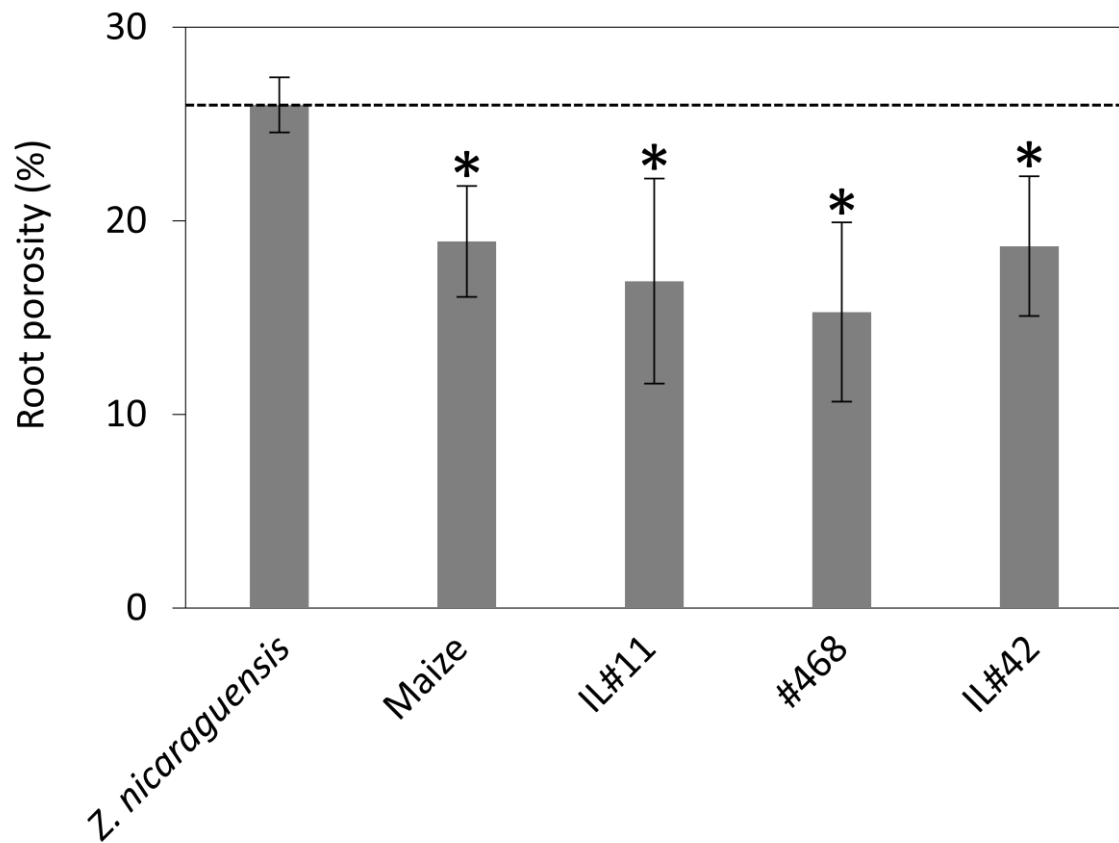


Figure S2. Whole root porosity (% , gas volume per unit root volume) of *Z. nicaraguensis*, *Z. mays* ssp. *mays* (maize), and introgression lines (ILs; *Z. nicaraguensis* chromosome segments in *Z. mays* ssp. *mays*) IL#11, #468 and IL#42. Plants were raised for 11 days and then grown for 2 weeks in stagnant deoxygenated solution. Values are means ($n = 4$) \pm SD. * indicates significant difference compared to *Z. nicaraguensis* ($p < 0.1$, one-way ANOVA and then Dunnett's test).

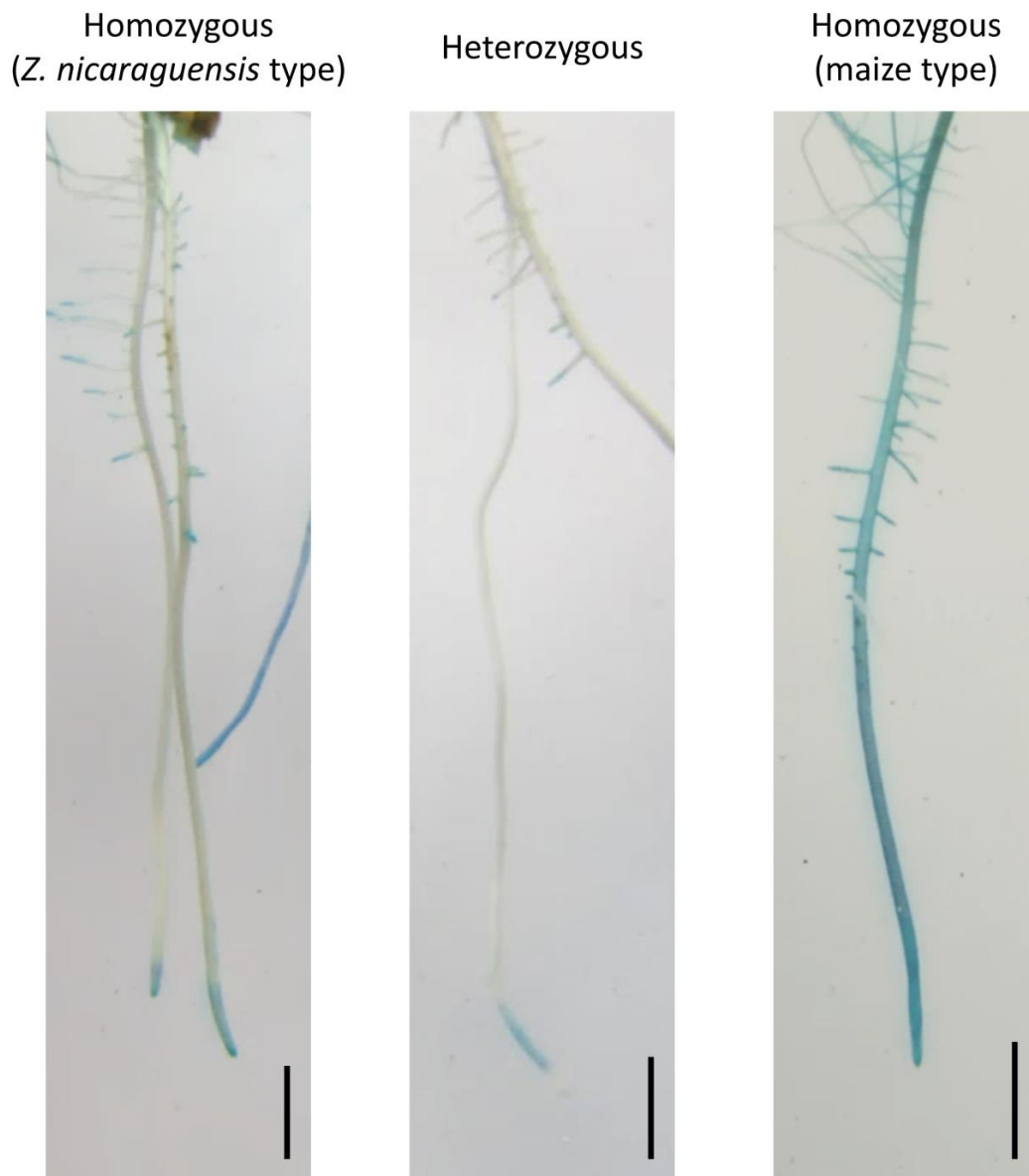


Figure S3. Evaluation of abilities of ROL barrier formation in adventitious roots of introgression line IL#11 plants possessing *Z. nicaraguensis*-derived chromosome 3 segment with homozygotes or heterozygotes or possessing the equivalent maize-derived chromosome segment by a methylene blue staining assay. Plants were raised for 11 days and then grown for 2 weeks in stagnant deoxygenated solution. Shoots were in air and roots were in an oxygen-free medium; blue indicates oxygen that has diffused outwards from within the roots. Bar = 1 cm.